A CLINICIAN LOOKS AT MRI

Basic MRI Physics

Diagnosis of Central Nervous System Infections

Clark R. Gregg, M.D.
Internal Medicine Grand Rounds
University of Texas Southwestern Medical School
August 3, 1995

Introduction

Over the last two decades we have seen a remarkable evolution of imaging techniques for central nervous system (CNS) infections. Routine radiographs of the skull remain valuable in assessing fractures, sinusitis, mastoiditis, and soft tissue calcifications, all of which have important implications for diagnosing intracranial infections. However, soft tissue contrast resolution of intracranial contents is not a feature of a routine radiographs. Standard tomography of sinuses and mastoids can enhance the value of routine radiographs but has been entirely eclipsed by computerized tomography (CT). Arteriography and venous angiography are occasionally useful in the evaluation of mass lesions of the brain and of cavernous sinus thrombosis but in practice are seldom the most crucial imaging studies applicable to clinical decision-making in consideration of CNS infections. Radioisotope techniques, which provide information on pathophysiology of focal lesions, are evolving in their breadth of clinical applicability but provide too little spatial or contrast resolution to compete with CT and magnetic resonance imaging (MRI) in practical daily value to the clinician. Without doubt the greatest technological leaps forward thus far in imaging CNS infections have been the development and further perfection of CT scanning since the 1970's and of magnetic resonance imaging in the 1980's and 1990's. CT imaging provides superior soft tissue contrast resolution compared to routine radiographic imaging but at a cost of inferior spatial resolution (Table 1). The spatial resolution of lesions with MRI is similar to that of CT, but MRI yields the best contrast resolution of all currently available methods. Soft tissue contrast resolution is one of the major advantages of MRI.

Table 1. Spatial and contrast resolution

Technique	Spatial Resolution (mm)	Contrast Resolution (mm)
Radioisotope	5	20
Radiography	0.1	10
CT	0.5	4
MRI	0.5	2

Computerized tomography, like other radiographs, depends on the relative attenuation of the x-ray beam by tissues of different electron density and atomic number. CT is unaffected by molecular motion or chemical interactions in tissue. Iodinated CT contrast media increase the attenuation of the x-ray beam and thus yield a brighter image in pixels where the contrast is concentrated. CT is limited to axial and, to a limited degree, coronal images.

MRI, on the other hand, involves physicochemical principles which are totally unrelated to CT. High contrast resolution of soft tissues derives from differences in the magnetic qualities of tissues. These variable qualities include differences in "spin" (proton) density and magnetic relaxation times of tissues as well as the bulk flow of protons in blood or cerebrospinal fluid. Tomograms are generated by application of radiofrequency pulse sequences in the presence of different external gradient magnetic fields which determine spatial encoding. The signals are interpreted and constructed into a digital image by computer. Manipulation of the pulse sequence parameters and gradient fields can yield tomograms with different information in any plane through the entire body.

Although all clinical training programs introduce principles of radiography, and these principles are rather straightforward, how MRI works is not straightforward and is not included in the usual curriculum for medical students or clinical physician residents. I am neither a radiologist nor a physicist, but I think that physicians who understand how MRI works will have an enhanced appreciation for disease processes and will be better able to understand the basis for a radiologist's interpretation of the images. Furthermore, with minimal knowledge of MRI physics, a clinician should be able to use the sequence parameters printed on the film to sort routine images for organized review on rounds or for conferences. A busy radiologist may not be available to assist conveniently in this process, and "T1", "T2", or "PD" are not always printed on the film, so it seems that the clinician should learn to perform these basic tasks for himself. This presentation is designed to introduce clinicians to fundamental MRI physics only insofar as is necessary to attain these practical goals. In fact, the details of MRI in daily application are extraordinarily more complex than in this review and appropriately reserved to the MR radiologist. It is beyond the scope of this discussion to cover the physics of newer techniques such as gradient echo, fast spin echo, and echo planar imaging, which in the future may supplant current conventional spin echo imaging. However, most contemporary clinical imaging of the CNS is still done using the conventional spin echo method, and this method I hope to make more clear to you. Several well written references (1-4) are available to the reader interested in learning more about MRI physics.

I shall also review the comparative CT and MRI findings in various CNS infections to illustrate the relative strengths and weakness of these different techniques. This information should assist clinicians in their use and appreciation of imaging technology in daily practice. Two unusually comprehensive and authoritative clinical reviews of CT and MR imaging of CNS infections (5, 6) are recommended for further reading.

MRI Physics

Nuclear Magnetism

Nuclear magnetic resonance was first described before World War II by Stern and Rabi, but Bloch (7) and Purcell (8) in the 1940's advanced our knowledge of NMR of solids which was ultimately the foundation for clinical MRI. Bloch hypothesized nuclear magnetism and developed mathematical equations to describe its behavior. NMR spectroscopy of material was in practical use by the 1960's, and the first application of NMR to imaging animals (9, 10) and humans (11) was in the 1970's. Because the word "nuclear" was so fearsome to lay people, the technique was renamed magnetic resonance imaging, or MRI.

Bloch described nuclear spin and its native property of creating a magnetic field, called a **nuclear magnetic moment**, along the spin axis (Fig. 1). Charged nucleons that contain an odd number of protons or neutrons (e.g. a hydrogen molecule or single proton) have an even stronger magnetic moment.

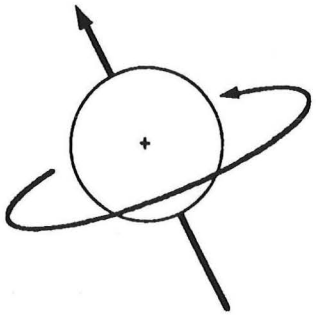

Fig. 1. Nuclear magnetic moment associated with the nuclear spin axis.

This magnetic dipole is a vector and will behave much like a minute bar magnet when placed into an external magnetic field. Conveniently, the hydrogen nucleus, a single proton, constitutes 80% of the atoms of the body, is found abundantly in water and lipids, and for these reasons and in part because of its high frequency of spin, yields the highest MRI signal of all the stable common nuclei. The ratio of the spin frequency to the nuclear magnetic moment of an isotope is called its **gyromagnetic ratio**, a value unique to each isotope and from which is calculated (see below) the radiofrequency (**RF**) pulse which will be used to induce resonance and thus generate an MRI signal.

Precession; Resonance Frequency

A spinning proton's magnetic moment has angular momentum, and, when placed into a strong magnetic field (called **Bo**) such as an MRI magnet will attempt to align with the axis of Bo. It's axis will also wobble around the Bo axis much like a gyroscope or top will wobble about its gravitational axis, a phenomenon call **precession** (Fig. 2).

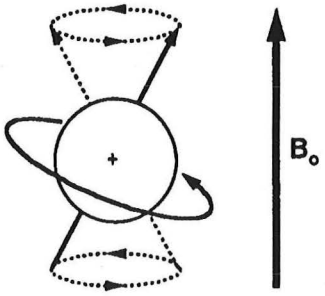

Fig. 2. A nuclear magnetic moment placed into a strong magnetic field precesses around the vector of the magnetic field.

The **frequency of precession** is the isotope's **resonance frequency** or so-called Larmor frequency and is the product of its gyromagnetic ratio and the strength of Bo. This is calculated by the Larmor equation:

$$\omega = \gamma \, Bo$$

in which ω is the frequency of precession (MHz), γ the gyromagnetic ratio of that isotope (MHz/T) and Bo the strength of the magnetic field in tesla (1 tesla (T) = 10,000 gauss (G)). Contemporary MRI superconducting magnets operate at 1.0 - 1.5 T. By comparison, the magnetic moment of the earth at the equator is only 0.3 G. The superconducting supercollider was projected to operate at 12T (1).

Precession and the precessional frequency are fundamental to understanding MRI. The precessional frequency is the frequency of the RF pulse that will be used to induce resonance in the protons to generate the MRI signal. By chance, the frequencies of RF pulses for MRI fall in the electromagnetic spectrum very near those of television or FM radio signals and hence are low energy non-ionizing radiation. In fact, the energy of an x-ray photon is 10 billion times that of a photon of RF radiation used in MRI. This inherent safety feature of MRI allows versatility in its application (e.g. pregnancy). The biologic effects of high strength magnetic fields and RF pulses are discussed later.

Nuclear Magnetic Resonance

The population of protons, or "**spins**" as they are called in MRI parlance, in the body is normally oriented randomly so their vectors cancel, and the body is nonmagnetic (Fig. 3).

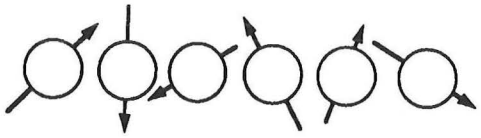

Fig. 3. Orientation of magnetic moments of protons with no external magnetic field.

However, these protons, when placed into the MRI magnet (Bo), will try to align parallel to Bo. Not all of the protons actually do so, and some of these, because of absorption of thermal energy, line up in the higher energy state antiparallel to Bo, but the net result is an ensemble of spins oriented parallel to Bo resulting in a **net magnetization vector (Mo)** parallel to Bo at equilibrium. Mo is directly proportional to the proton density in the tissue and to the strength of Bo (Fig. 4).

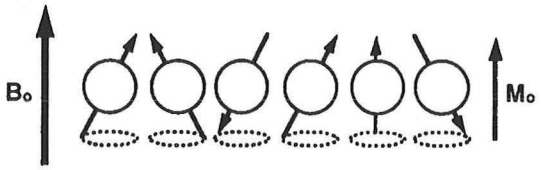

Fig. 4. Orientation of magnetic moments of protons when placed in a strong external magnetic field.

The time it takes to achieve this equilibrium will be described by the **T1 relaxation time** (see below) characteristic of that tissue. By convention, the external magnetic field Bo is assigned the Z axis in Cartesian coordinate vector diagrams describing MR phenomena. This is also called the **longitudinal** axis, whereas vectors in XY plane are said to be **transverse** (Fig. 5).

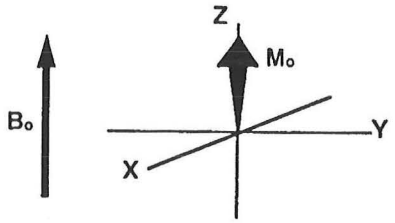

Fig. 5. Net magnetization vector of protons (Mo) at equilibrium is assigned the Z (longitudinal) axis. Vectors in the XY axes are called transverse.

A static magnetic vector such as Mo at equilibrium is not directly measurable. If, however, this vector can be tipped into the XY axes, it can be measured, because a moving magnetic vector will induce an electromagnetic signal in a nearby antenna. Thus we irradiate the protons with an RF pulse perpendicular to Mo at the precessional frequency of protons, causing them to absorb this energy. Two important results occur: (a) the net magnetic vector tips out of the Z axis and into the XY axes where it can be detected (Fig. 6),

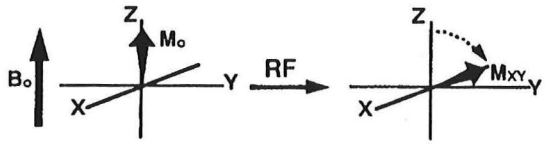

Fig. 6. The radiofrequency (RF) pulse induces magnetic resonance in the protons, tipping their net magnetization vector into the XY axes, where it is measurable.

and simultaneously (b) all of the precessing nuclear magnetic moments are brought into phase coherence (pointing in the same direction) (Fig. 7).

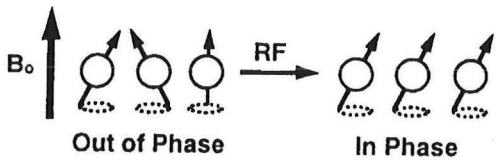

Fig. 7. The RF pulse also brings the precessing nuclear magnetic moments into phase coherence of their precessional cycles.

This phenomenon is **nuclear magnetic resonance**, and the result is a **net magnetic vector in the XY plane precessing about the Z axis at the resonance frequency** (Fig. 8). This net transverse vector precessing about the Z axis generates the MRI signal in the receiver antenna.

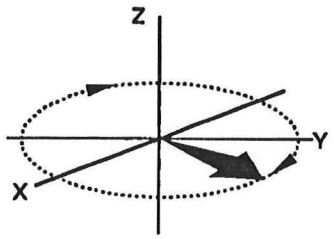

Fig. 8. At the end of an RF pulse, there is a net magnetic vector in the XY plane, precessing about the Z axis at resonance frequency. This moving magnetic vector generates an oscillating electromagnetic signal.

Depending on the strength and duration of the RF pulse, the net magnetic vector M can be tipped to any angle, but commonly 90° ("saturation recovery") and 180° ("inversion recovery") pulses are used. Small tip angles ("partial saturation") are used for rapid sequence imaging increasingly utilized recently. The physics of these more complex rapid sequence images will not be discussed in this presentation.

Free Induction Decay, the Basic MRI Signal. T2 and T1 Relaxation

Following cessation of a saturating RF pulse, the XY (transverse) magnetization vector immediately begins to decay as the individual proton magnetic moments dephase and return to the equilibrium distribution of precessions about the Z axis and flip back to the lower energy state in alignment with Bo. This dephasing occurs not only because of interactions of the spins with nearby magnetic fields of other nuclei (which is what we are trying to measure) but also because of inhomogeneities of the MR magnet (this is important and will be recalled later). This decay of transverse magnetization occurs in a spiral fashion which describes an oscillating signal in the fixed receiver antenna in the XY plane. This signal, plotted against time, is the **free induction decay (FID)** and is the basic MRI signal (Fig. 9).

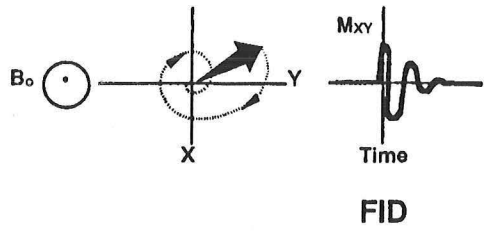

Fig. 9. Viewed from above, the precessing transverse vector decays in a spiral. An antenna in the XY plane detects an oscillating signal, the free induction decay (FID), which is the basic MRI signal. This decay occurs at the T2 relaxation rate for that tissue.

This decay of transverse magnetization proceeds at a rate characteristic for that tissue called the **T2 relaxation** rate. The T2 value for a tissue is the time it takes for 63% decay of transverse magnetization. Differences in signal strength from tissues will occur because of their intrinsic differences in T2 relaxation rate (Table 2).

Simultaneously, but independently from T2 relaxation and at a different rate (slower), net magnetization in the Z (longitudinal) axis regrows following cessation of the RF pulse. This rate can be measured indirectly and is described by the **T1 relaxation** rate (Fig. 10).

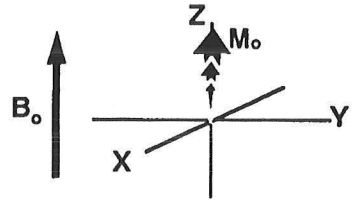

Fig. 10. Longitudinal relaxation regrows independently and more slowly than transverse relaxation. This return to equilibrium (Mo) is described by the T1 relaxation rate.

The T1 value for a tissue is the time it takes for 63% recovery of longitudinal magnetization. T1 also differs among tissues and is the basis for contrasting signals on T1-weighted images (Table 2). The signals generated from tissues for both T1- and T2-weighted images depend for their intensity on the concentration (density) of mobile protons in the tissue. This is why air (sinuses, mastoids, etc), bone, and calcifications, which lack mobile protons, yield no MRI signal.

Table 2. T2 and T1 relaxation times; Bo = 1.0 T

Tissue	T2 (ms)	T1 (ms)
Fat	90	180
White matter	90	390
Gray matter	100	520
Blood	180	800
CSF	300	2000
Water	2500	2500

Adapted from (1)

Soft Tissue Contrast Derived from Differences in T1 and T2

Contrast between tissues can be imaged by taking advantage of differences in T1 and T2 values. More rapid T1 relaxation (shorter T1 time) results in a stronger (brighter) T1 signal. Fat has a short T1 and a bright signal, whereas CSF and edema fluid have long T1 and a darker signal on **T1-weighted images (T1WI)**. T1 of diseased or damaged tissue, because of edema (water, protein) has long T1 and thus a lower signal intensity than healthy tissue. In general, then, T1WI are best for definition of **normal anatomy** and for use with paramagnetic **contrast agents**, which act by shortening T1 (brighter signal) at foci where they are concentrated. Paramagnetic contrast agents are discussed later.

With **T2-weighted images (T2WI)**, on the other hand, tissue with long T2 such as CSF will appear bright (persistent transverse magnetization = more signal) and that with short T2 will appear darker. Diseased or damaged tissue (edema) will often have longer T2 than healthy tissue and thus a higher signal intensity on T2WI (the opposite of T1WI). Therefore, because hyperintense signals are more easily appreciated visually than hypointense signals, T2WI are generally better than T1WI for discovering **pathology**.

MRI Tomography: Gradient Magnetic Fields

Tomography using MRI is accomplished by the application of additional external gradient magnets along the Bo axis. This gradient focuses the location and thickness of a slice by modulation of the proton resonance frequency in a slice to match identically the frequency of the RF pulse. Protons in tissue outside this focussed slice along the gradient will have different resonance frequencies and will not be stimulated by the RF pulse, thus yielding no signal. Spatial encoding of a pixel within a slice is determined by application of additional external gradient magnets at right angle orientations.

MRI in Practice: The Spin-Echo Sequence; TR and TE

How are MRI signals actually obtained in practice and translated into **T1WI**, **T2WI**, and **proton density weighted images (PDWI)**? Recall that the basic MRI signal is the **free induction decay (FID)** and that it oscillates to zero quickly as a result of dephasing of proton precessions. Recall also that this dephasing was in part a function of imperfections in the MRI magnet, which cause some protons to precess faster or slower than others and lose phase coherence. This artificial dephasing can be compensated for by use of what is called a **spin-echo sequence** and a signal more reflective of actual tissue relaxation obtained. Following a 90° RF pulse, protons that dephase because of magnetic field inhomogeneity (imperfections in the magnet) can be rephased by application of a 180° RF pulse which effectively reverses the order of the precessions (Fig. 11).

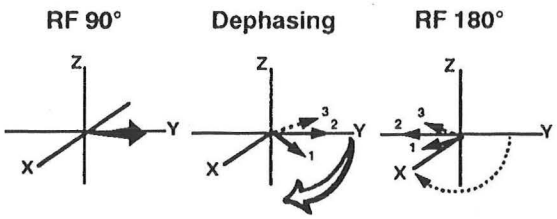

Fig. 11. A 90° RF pulse is followed by dephasing of proton precessions. Those that dephase because of magnet imperfections will be rephased by a 180° RF pulse which reverses their order, allowing faster precessions to overtake slower ones. A true T2 signal can then be measured.

The same faster-precessing protons will then overtake the slower-precessing protons, coming back into phase, generating what is called a **spin-echo** signal, which is more easily measured than the FID and whose peak is a true indication of the underlying state of T2 relaxation at that time. The conventional spin-echo is the signal actually measured in most common clinical MRI applications. The time from the 90° RF pulse to the peak of the spin-echo is called the **time to echo**, or **TE**. The measurements are taken as a series of grouped pulses called a pulse sequence. The time from the 90° pulse to the next 90° RF pulse in the sequence is called the **repetition time**, or **TR** (Fig 12). The importance to you of **TR** and **TE** is discussed below.

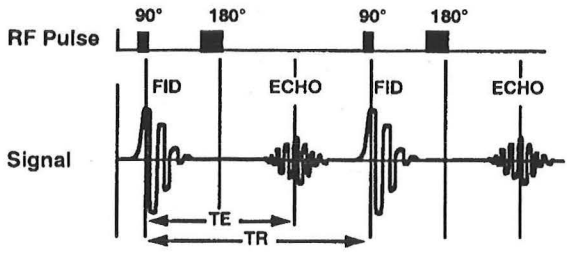

Fig. 12. A 90°-180° pulse sequence generates a spin-echo. The time from the 90° RF pulse to the peak of the echo is the time to echo (TE). The time between 90° pulses in the sequence is the time to repetition (TR). Manipulation of TR and TE results in the T1-, T2-, or proton density weighted images.

Importance of TR and TE

Manipulations of TR and TE allow the radiologist to generate **T1-**, **T2-**, or **proton density weighted images** (sometimes also called spin density weighted images, or SDWI). TR and TE values are printed on the image film, and by knowledge of these values the reader can tell which type of image he is viewing. If TR is sufficiently long (e.g. 2000 ms) to allow nearly full T1 relaxation of all tissues before the next 90° pulse, the echo signal following the next pulse will largely reflect only proton density, minimizing T1 contrast. If then TE is very short (e.g. 20 ms) so as not to allow time for significant T2 relaxation of the tissues, the spin-echo signal obtained will also largely reflect proton density. Therefore, a **long TR - short TE** spin-echo pulse sequence results in what is called a **proton density weighted image (PDWI)** (Table 3).

If TR is set long as with PDWI, but TE is set longer than with PDWI (e.g. 80 ms) to allow time for separation of the T2 relaxation curves of contrasting tissues, the spin-echo signal obtained will reflect not only proton density but also T2 contrast. The latter is more important in these images, and therefore the **long TR-long TE** spin-echo pulse sequence yields a **T2-weighted image (T2WI)** (Table 3).

The largest separation (contrast) between the T1 relaxation curves of two tissues is at the time average of the T1's of those tissues. If TR is set near that average (e.g. 300-1000 ms), at the second and subsequent 90° pulses T1 relaxation will have occurred more in some tissues than others, and the differences in signal strength of the tissues will in large measure be a function of differences in T1. TE is set short to minimize T2 effects so that the resulting spin-echo signal reflects T1 contrast and proton density differences. The contribution of T1 differences is greater, so these **short TR-short TE** images are called **T1-weighted images (T1WI)** (Table 3). Bear in mind that T1, T2, and PD contribute something to each image, regardless of weighting toward one or another.

Table 3. Typical spin-echo pulse sequences

Weighting	TR (ms)	TE (ms)
PD	>2000	<40
T2	>2000	>80
T1	300-1000	40-80

With knowledge that you now have of what the TR and TE values in conventional spin-echo signify, you should be able to find those values printed on the film and sort a stack of MR images into their respective groups by weighting. This skill will allow you to organize your review of the images and better appreciate the MRI signal characteristics of both normal and pathologic tissue.

Imaging Osteomyelitis: STIR Sequence Images

A disadvantage of MRI compared to other techniques such as CT is the failure of bone, because of its paucity of mobile protons, to produce an MRI signal, resulting in a signal void. As a result, MRI is not the best technique to image the destruction of bone by infection, tumor, etc. However, the bone medulla contains marrow fat which yields a signal. Osteomyelitis results in accumulation of inflammatory edema in the medullary cavity which may be difficult to image by conventional spin-echo techniques because of the contiguous fat signal. A special pulse sequence called **STIR** (**s**hort **t**ime **i**nversion **r**ecovery) can be used to nullify the fat signal. The image that results reflects additive T1 and T2 signal from the inflammatory edema and effectively discovers the extent of the lesion. It is not essential for the clinician to understand the physics of STIR sequence imaging, but it may be useful to discuss with the radiologist obtaining this study if you are evaluating diabetic foot infections, vertebral infections, or other problematic bone/soft tissue infections.

MRI Detection of Hemorrhage

Some intracranial infections are characterized or complicated by petechial or gross hemorrhage. Infections most notably associated with intraparenchymal hemorrhage include infective endocarditis; early brain abscess; tuberculous meningitis; invasive aspergillosis and other filamentous fungal infections; herpes simplex encephalitis; Listeria monocytogenes cerebritis/rhombencephalitis; cortical hemorrhage complicating bacterial meningitis or septic dural venous sinus thrombosis; and CNS toxoplasmosis complicating AIDS. With the advent of high field strength MR magnets in the last ten years, the detection and characterization of intraparenchymal CNS hemorrhage have been extensively investigated and described.

The appearance of acute hemorrhage on CT scan is due to the focal concentration of electron-dense protein, but within days these changes generally fade away. Moreover, hemorrhage associated with infections is often petechial and does not result in a large enough focal accumulation of blood to be detectable by CT. By comparison, the changes characteristic of hemorrhage on MRI depend on the magnetic qualities of hemoglobin and its metabolic products, and typical abnormalities attributable to hemorrhage may remain for years. MRI is a considerably more sensitive technique than CT for detecting small subacute or older hemorrhages, and the evolution of the MRI appearance of hemorrhage in sufficiently described that the radiologist can roughly guess the age of the bleed.

The key to understanding the MRI appearance of hemorrhage is the metabolic status of hemoglobin and its associated iron (12, 13). Iron in oxyhemoglobin is in its ferrous (Fe^{++}) form, has no unpaired electrons in its outer shell, and thus is diamagnetic (does not influence T1 and T2). Atoms with unpaired electrons are called **paramagnetic** and can influence the spin relaxation times of nearby protons. Deoxyhemoglobin (four unpaired electrons) is mildly paramagnetic, and methemoglobin, in which the iron is ferric (Fe^{+++}), is more so because of its five unpaired electrons.

Acutely after a hemorrhage, the MRI signal on T2WI will be that of central hypointensity because of the T2 shortening effects of deoxyhemoglobin, surrounded by an area of hyperintensity typical of edema. T1WI may show very little. In subacute hemorrhage (3-7 days old), deoxyhemoglobin has been denatured to methemoglobin, and its iron oxidized to Fe^{+++}, which **shortens the T1 time** of nearby water protons, resulting in a bright signal on T1WI. This T1 effect of methemoglobin is one of few pathologic processes resulting in a bright signal on noncontrasted T1WI and is a hallmark of subacute hemorrhage. Since such foci of hemorrhage, especially if inflammatory, may also show contrast enhancement with gadolinium chelates (see below), it is important also to study the noncontrasted T1WI so that the changes attributable to hemorrhage will not be mistaken or overlooked. There are other evolutionary MRI changes following hemorrhage (12, 13), but they are beyond the practical scope of this review pertaining to infections.

MRI Contrast Agents

Background

One of the major advantages of MRI compared to other available imaging modalities is its ability to detect subtle contrast in soft tissues. In this regard, MRI was originally thought to be so sensitive that contrast agents would not be necessary (14). However, in the last decade, and especially since the FDA approval in 1988 of gadopentate dimeglumine (Magnevist) for clinical use in the United States, extensive study and experience with paramagnetic contrast agents have established a broadly accepted role for their selective use (1, 15-17). By some estimates, 70% of MRI studies of the brain and 25% of studies of the spine now include the use of contrast agents. MRI contrast agents may in some situations add not only some sensitivity of detection of pathology but also specificity (15-17). Although there is some debate about indications for the routine use of contrast enhancement (16, 17), there seems to be consensus in the radiology literature that contrast agents should always be used in evaluating possible inflammatory conditions of the central nervous system (15, 18). Effective MRI contrast agents for abdominal and gastrointestinal studies can be administered by mouth, but to date the only clinically useful contrast agents to study CNS disease are intravenously administered metal ion chelates.

How Paramagnetic Contrast Agents Work

In conventional radiography including CT, contrast agents directly attenuate the x-ray beam in tissues where the contrast is concentrated. MRI contrast agents are not themselves visualized but rather alter the relaxation times of nearby protons, resulting in an altered signal compared to noncontrasted studies (15, 19). It follows that the most effective contrast agents are those that modify the proton relaxation times the most. The magnetic attributes of an atom are in large measure dominated by the effects of unpaired electrons in the outer shell, which have much more powerful magnetic dipole moments than protons (19). Atoms with the most unpaired electrons such as the transitional and lanthanide metals thus have the strongest magnetic effects. Gadolinium (Gd^{+++}) has seven unpaired electrons whereas transitional metals such as iron, manganese, and chromium have fewer. Moreover, all these metals are toxic in their elemental form, so they must be chelated to render them safe for biologic use. When transitional metals are chelated, their proton interactive sites are all occupied or obscured. Only the lanthanides such as gadolinium retain enough proton interactive sites to remain magnetically effective after chelation (19), and thus gadolinium has been the most widely used metal for the production of intravenously administered MRI contrast agents.

Gadolinium is normally nonmagnetic but under the influence of an external magnetic field is somewhat magnetic, a trait known as **paramagnetism**. In the MRI magnet, paramagnetic elements exert a strong local magnetic effect on protons that pass nearby, which shortens both T2 and T1 relaxation times (19). The effects on the images are those of a **brighter signal on T1WI** and a darker signal on T2WI. At low concentrations of paramagnetic contrast agents used in clinical radiology, the T1 effects are much more striking than the T2 effects (14, 19), and thus T1-weighted images are used to visualize contrast enhancement at sites of breakdown of the blood-brain barrier.

Why Use Contrast in MRI?

Normal structures in an about the brain and spinal cord do not enhance with gadolinium chelates, with the exceptions of the pituitary infundibulum, pituitary gland, cavernous sinus and some other vascular structures, choroid plexus, the pineal gland, and occasionally the dura mater (14). Enhanced MRI in infectious conditions of the CNS is most useful in defining inflammatory mass lesions such as parenchymal, subdural, or epidural abscesses and in detecting meningitis, especially basilar meningitis (18). Contrast is also useful in detecting periventricular or parameningeal cortical inflammation which might otherwise be difficult to distinguish from the bright signal of the contiguous CSF on T2WI (14). Contrast enhancement of a lesion, or lack thereof, is also important in differentiating various CNS diseases that complicate HIV infection (18), as will be discussed below. Highly vascular tumors exhibit contrast enhancement and MRI has been very sensitive in detecting drop metastases in the meninges (14, 15, 20), a problem with which infectious diseases are often in the differential diagnosis.

Properties of Current Contrast Agents

Three MRI contrast agents are currently available in the United States, whose brand names are Magnevist (gadopentate dimeglumine), ProHance (gadoteridol), and Omniscan (gadodiamide). These differ in chemical qualities including linear vs. macrocyclic and ionic vs. nonionic (21), but all are equivalent in clinical efficacy and safety (1). Nonionic macrocyclic compounds such as ProHance are theorized to have fewer adverse effects, but in clinical studies and extensive practice none of the gadolinium chelates has been associated with a significant incidence of adverse reactions (1, 22-24). They are all distributed rapidly into the blood and extracellular fluid

spaces and are eliminated within hours by glomerular filtration (1, 14, 21). They cross the placenta and have been detected in the fetal bladder. Otherwise they are nonspecific for any particular organ on lesion distribution. Their value in imaging CNS lesions is that they accumulate at sites of interruption of the normal blood-brain barrier. A decision on which agent to use in a diagnostic imaging center is often made on economic considerations.

Adverse Effects

Adverse effects of MRI contrast agents are unusual and generally minor, including headache, nausea, vomiting, hives, and local hot or cold sensations at the injection site. Magnevist has been associated with transient rises in serum iron and bilirubin levels, suggesting hemolysis, but there have been no problems with the agent in patients with hemolytic anemia or sickle cell disease (25). Anaphylactoid reactions have occurred but are rare. Extravasation of these hyperosmolar solutions at the injection site may result in phlebitis or soft tissue sloughing.

Trace metals in the blood such as zinc or copper may displace some gadolinium from its chelate, resulting in a plasma concentration of free gadolinium. So far these gadolinium levels have been low and the ion cleared rapidly, not associated with adverse effects, but what influence renal failure or illnesses such as Wilson's disease might have on gadolinium levels has not been entirely worked out (25). In general, these agents are considered safer than iodinated x-ray contrast media for patients with renal disease.

Safety Issues in Magnetic Resonance Imaging

For several decades there has been a great deal of interest in the biologic effects of high strength magnetic fields. Although early studies showed no deleterious biological effects of static fields of less than 5.0T (26), the development of clinical MRI in the late 1970's engendered increased interest in the possible adverse effects of this new technology. Attention was given to the effects of not only static magnetic fields but also rapidly changing magnetic fields and radiofrequency pulse sequence applications which are used in MRI.

Static and Gradient Fields

A review by Budinger (27) concluded that there was no scientific evidence for detrimental effects in humans from exposure to static magnetic fields up to 2.0 T. Later reviews (1, 25) confirm the apparent safety of static magnetic fields. There are, however, potential effects of rapidly changing magnetic fields as might be experienced in the switching on and off of gradient magnets. These potential effects include visual light flashes (called magnetic phosphenes) and cardiac fibrillation, but the current density induced by clinically applied early MRI devices did not approach the thresholds for these phenomena (27). Later study of more advanced fast-oscillating gradients similarly showed that these oscillating magnetic fields induced currents that were still far below cardiac fibrillation threshold (28). A recent review (25) also dispels this concern.

Radiofrequency Pulse Exposure

Radiofrequency pulse radiation, on the other hand, has been of concern because of the tissue heating that occurs on absorption of this energy, analogous to microwave cooking. Although early clinical studies detected no adverse effects of MRI (29) using low field strength magnets and low energy RF pulses compared to today's machines, international guidelines were developed to limit the whole body specific absorption rate (SAR) of energy (30). Subsequent studies using

SAR's exceeding these guidelines showed some rise in body and skin temperatures but no apparent deleterious or symptomatic short term effects (31). Later, however there have been reports of first-, second-, and third- degree burns as a result of MR examinations of patients with cutaneous monitor wires or other conductor contacts (25, 32). Although there have been concerns that tissue heating might have adverse effects on spermatogenesis or might cause cataracts, so far these fears have not been realized (25). Modern MRI machines calculate the SAR and do not allow the examiner to override permissible limits (1).

Ferromagnetic Objects, Devices, and Materials

Much more of a daily issue than any of the above is the influence of the magnetic field on ferromagnetic implants or foreign bodies in patients and the risk that ferromagnetic objects in proximity to the MRI magnet might be attracted forcefully into the magnet, thus possibly injuring patient or staff. Shielding the magnet to limit fringe magnetic fields might actually increase the hazard by damping the early warning provided by a weaker fringe field (25). Metal detectors are too insensitive to detect such subtle but potentially dangerous objects as cerebral aneurysm clips or metallic foreign bodies in the eye, either of which could torque on entering the magnetic field and cause serious damage (25).

Magnetically sensitive implanted devices such as cardiac pacemakers, implantable defribrillators, or insulin pumps will malfunction when brought into the magnetic field. Pacemakers include a reed relay switch which is actuated magnetically to allow asynchronous operation of the pacemaker. Reed relay switch closure occurs at very low magnetic field strength and may occur far out in the fringe magnetic field distant from the scanner (1, 25). Concern has also been raised as to the possible risk of electrical conductivity of pacemaker wires or derelict epicardial pacer wires from previous cardiac surgery, which might serve as antennae for electromagnetic currents induced by MRI and provoke arrhythmias. Cardiac deaths have occurred during MRI of patients with pacemakers, and thus pacemaker patients are systematically prohibited from MRI study (1, 25).

Alloys that contain iron, nickel, or cobalt are often ferromagnetic and thus susceptible to magnetic fields. Metal intracranial aneurysm clips, shrapnel injuries, and intraocular metal foreign bodies are particularly risky for patients subjected to MRI, and so these patients are best excluded from study. Depending on their construction and alloy composition, medical implants or equipment that are called surgical stainless steel may or may not display ferromagnetism (1, 25). Surgical clips manufactured since 1980 have all been non-ferromagnetic, but it is often difficult to tell whether a patient has these modern clips in place. Similarly, prosthetic heart valves manufactured since 1982 are non-ferromagnetic and safer (1). In 1988, Shellock compiled the published reports on the ferromagnetic qualities of a large variety of metallic implants, devices, and materials used in health care (33). Although many of these did exhibit magnetic deflection in relevant field strengths, most were considered safe for MRI exposure because those deflections were minimal compared to forces the devices or material encounter in situ. Bushong (1) tabulated implantable devices which raise eyebrows among MRI operators and may be a contraindication to MR imaging including the electrical devices mentioned but also cochlear implants, dental implants, ocular implants, orthopedic implants, penile implants, metallic intravascular or gastrointestinal stents, hemostatic clips, and halo vests. A recent comprehensive review by Kent, et al (34) considers cochlear implants a definite contraindication to MRI. Even if generally considered safe, such objects may nonetheless create imaging artifacts.

Various ferromagnetic objects can become dangerous projectiles in the strong field of attraction of an MR imaging magnet (Table 4). In daily practice, physicians, nurses, porters, attendants,

housekeeping personnel, and patients or their family or friends may inadvertently transport such objects into the MRI suite and create a very dangerous risk to patient and personnel, let alone damage to the very expensive MRI equipment. Many tragic injuries have occurred because of such recognizable but overlooked hazards, and thus MRI personnel are trained to be exceptionally vigilant to avert these dangers. Physicians and nurses should also screen patients before sending them for MRI exam to be sure all jewelry, prostheses, hearing aids, and other metallic objects are left behind. A review of Table 4 will suggest to the reader a multitude of other common devices and objects which might similarly create a projectile hazard.

Table 4. Ferromagnetic objects and devices reported either as projectiles in or influenced by MRI magnets.

Personal items		
calculator	key	pen
clipboard	knife	pencil
film magazine	lighter	steel tipped shoes
hairpin	magnet	tools
ID badge	nail clipper	watch
jewelry	paper clip	
Housekeeping or physical plant items		
bucket	forklift tines	vacuum cleaner
buffing machine	mop	
fan	tile cutter, roller	
Medical devices or equipment		
ankle weights	MR table parts	"sand" bag (iron pellets)
chest tube stand	oxygen tank	scissors
gurney	pacemaker	stethoscope
hearing aid	pager	surgical instruments
insulin pump	prosthetic limb	wheelchair
IV pole	pulse oximeter	

Compiled from (1, 25).

Auditory Effects

The rapid switching of the gradient magnets results in a loud banging noise at 65-95 dB, which may rarely result in temporary or permanent hearing loss (25). Phase cancellation techniques are being studied and may be helpful, but headphones or earplugs are presently more practical.

Psychological Effects

Claustrophobia, anxiety, panic and other usually transient adverse psychological consequences of placement into the confines of the MRI magnet core occur in 5-10% of patients (25). Various ways to comfort patients through the examination may be attempted, including allowing a friend or family member to remain with the patient.

Pregnant Patients or Personnel

Although there have been no reports of adverse outcomes of pregnancy as a result of exposure to

magnetic resonance imaging or its environment, nonetheless radiologists are cautious about potential risks to pregnant patients and personnel. Some tissue heating occurs as a result of absorption of energy from the RF pulses, and heat is teratogenic. However, the heating that occurs is no more than would be expected from a hot tub or heating pad (1). MRI is considered not as safe as ultrasound examination but safer than CT scanning or other standard radiographic techniques, and thus MRI is safely performed in pregnancy after careful consideration of the medical necessity of the procedure. Current consensus opinion is that paramagnetic contrast agents be avoided in pregnancy (34).

Technologists working in the fringe magnetic field of the MRI device are exposed to field strengths comparable to household magnets. They are not exposed to the switching gradient fields or RF pulses. Pregnant personnel are nevertheless advised to remain outside the 10 G range of the static magnetic field and avoid unnecessary proximity to the MRI machine during activation of the gradient fields and RF pulses (25).

Imaging Central Nervous System Infections

Should I Order a CT Scan or an MRI?

Computerized axial tomography and magnetic resonance imaging have revolutionized our diagnostic approaches to neurological disease to the extent that no neurological workup seems complete, or even started, without acquiring one or the other or both. However, major critical reviews of published studies on the tangible impact of MRI on diagnostic accuracy, medical decision-making, patient outcomes, and cost-effectiveness suggest that the supporting evidence for many clinical uses of MRI is quite weak (34, 35). On the basis of these reviews, the American College of Physicians has on two occasions published position statements on the use of MRI in clinical medicine to serve as practice guidelines (36, 37). A sampling of the case series and review literature on the use of MRI in CNS infections quickly indicates the degree to which MRI has been acknowledged and accepted as superior in sensitivity compared to CT scanning for many infectious diagnoses (5, 6, 38-43). Is this confidence in MRI justified?

In their exhaustive assessment of the peer-reviewed medical literature from 1987 through 1993 on MRI in neuroimaging that was the basis for the 1994 ACP position statement, Kent, et al, culled 3125 citations down to 325 original-data papers worthy of further review (34). They classified those studies as to quality of methodology according to stringent criteria and focussed on the 156 that addressed accuracy, diagnostic and therapeutic impact, or patient outcomes. Finally they rated these studies on an A through D scale according to internal validity and external generalizability according to prospective criteria. They cited only nine papers pertaining to infection of the nervous system, one of which was a review of MRI in spinal infections, concluding that there were no published studies that they could rate grade C or better. That is, all studies had multiple methods flaws, selection bias, and opinion without substantiating data. Based apparently on prevailing expert opinion, however, they concluded the following: (a) MRI is the study of choice for imaging infections and inflammations of the spine; (b) MRI is considered the most sensitive imaging modality for detection of infections and neoplastic complications of advanced HIV infection and AIDS; (c) the use of paramagnetic contrast agents should be reserved for unusual lesions, because their use does not commonly alter diagnostic decisions or treatment plans; and (d) no study has reported improved patient outcomes as a result of the application of MR imaging (34).

Based on this study, the same authors prepared the ACP's revised position statement on behalf of the College's Health and Public Policy Committee which was published simultaneously. They concluded that, "Although studies of MRI for infections have been small case series that only showed image quality, MRI is now the preferred test for brain infections" (37), despite the finding that the supporting evidence is weak to equivocal. CT scanning is sufficient to exclude mass lesions prior to lumbar puncture, but MRI is superior in evaluation of neurologic syndromes associated with HIV infection. For the seriously ill patient, the test to order is the one that can be obtained more promptly (37).

The comparative advantages of MRI over CT scanning thus can be summarized as follows:

(a) improved soft tissue contrast without bone artifacts;
(b) images of equal clarity in any orientation;
(c) no exposure to ionizing radiation and thus safe for pregnant patients;
(d) usually does not require contrast to make appropriate interpretations; and
(e) paramagnetic contrast agents are probably safer than iodinated contrast agents used in CT scanning.

On the other hand, CT scanning has the following advantages over MRI:

(a) data acquisition is faster;
(b) less patient cooperation is required;
(c) life support systems can be used in the scanner;
(d) ferromagnetic foreign bodies, materials, and implantable devices are not contraindicated (but they create imaging artifacts);
(e) bone lesions and calcifications are detectable;
(f) contrast agents are generally safe and adequate for most infection indications; and
(g) it is less expensive.

Pyogenic Infections

Acute Meningitis

The diagnosis and management of acute viral meningitis and uncomplicated acute bacterial meningitis are generally straightforward, and imaging studies are usually unnecessary. Moreover, CT and MRI studies generally yield normal results in these situations (6, 44). CT or MRI may, however, be useful in severe or complicated pyogenic meningitis by detecting focal complications, suggesting alternative diagnoses, and defining parameningeal foci such as mastoiditis or sinusitis from which infection may have originated. In subacute or localizing neurologic syndromes which may suggest brain abscess, either CT or MRI is useful to exclude a mass lesion prior to performing a lumbar puncture.

An often subtle early radiographic sign of acute bacterial meningitis is distension of the sulci over the convexity of the brain (45), but this finding may be difficult to appreciate in older adults because of possible underlying cerebral cortical atrophy (5). Nonetheless, because of its superior resolution of anatomic detail, MRI is superior to CT in detecting this abnormality, and T2WI and enhanced T1WI offer the most information (38, 44).

In an animal model of acute pyogenic meningitis, inflammation of the pia-arachnoid occurred within hours to days of inoculation of bacteria (46). Gadolinium-enhanced MR imaging was more sensitive than contrast-enhanced CT scanning at detecting this inflammation and correlated well with histopathologic findings. However, the thickness of the dogs' skulls degraded the quality of the CT images, making the comparison less compelling. Clinical experience and studies of meningitis in humans have confirmed the sensitivity of MRI compared to CT in detecting meningeal enhancement (5, 44). Meningeal enhancement, which may be striking, does not indicate a worse prognosis (5) but may be slow to resolve. Dural enhancement, which is occasionally a normal finding, differs in appearance from pia-arachnoid enhancement by its conformity to the inner surface of the skull rather than to the gyri and sulci of the cerebral cortex.

Cerebritis and cortical infarctions are serious complications of acute pyogenic meningitis that result from vasculitic occlusion of the small arteries or veins that traverse the subarachnoid space (47). This may be further complicated by vasospasm of larger deep arteries and infarction of large segments of cerebral cortex. Occlusion of major dural venous sinuses may result in multifocal hemorrhagic infarction of white matter (6). Arterial occlusions appear typical of infarcts on CT scan, and many show subtle delayed enhancement. MRI shows high intensity signal on T2WI, often with mass effect. Unenhanced T1WI may show evidence of petechial hemorrhage, especially if there is cortical venous occlusion, and studies using contrast agents usually show focal enhancement (5). The finding of a focally high signal rather than the usual signal flow void in a venous sinus or artery on unenhanced T1WI should suggest thrombosis of the vessel (5, 6, 43).

Ventriculitis may follow placement of a ventriculoperitoneal shunt and often complicates bacterial, especially Gram-negative bacillary (48-50), meningitis. In an animal model of acute bacterial meningitis, contrast-enhanced MRI detected ventriculitis, but CT did not (46). In humans, evidence of ventriculitis that can be appreciated on CT scan includes indistinctness of the ependyma, irregularity of the margins of the ventricles, subependymal edema, hydrocephalus, and perhaps subtle increase in radiodensity of ventricular fluid (5). Ependymal inflammation results in contrast enhancement with CT or MRI, but these changes are more sensitively detected with MRI. Periventricular edema is best appreciated on T2WI, but the proteinaceous ventricular fluid is most distinguishable using T1WI (brighter signal than normal CSF because of shorter T1) (43). T1WI with gadolinium enhancement also detects periventricular inflammation.

Subdural effusion (hygroma) or, less commonly but more importantly, subdural empyema may complicate bacterial meningitis, especially in infants (51). By CT scan, both appear hypodense and may be difficult to appreciate because of interfering skull bone artifacts. These effusions are more easily appreciated using MRI, and also MRI can help distinguish hygroma from empyema. Hygromas do not enhance and are isointense to CSF by T1WI and T2WI, whereas, and analogous to changes in ventriculitis, the highly proteinaceous empyema fluid is brighter than CSF on T1WI and hyperintense compared to brain and CSF on T2WI and PDWI (6, 52, 53). The limiting capsule and surrounding inflammation enhance with contrast by either CT or MRI (5).

Subdural and epidural empyemas more commonly occur as a result of contiguous paranasal sinusitis or mastoiditis, but also may complicate trauma, prior neurosurgery, or bacteremia (51, 54). MRI is more sensitive than CT at detecting and determining the extent of these empyemas as well as somewhat more sensitive at detecting other corroborative findings such as underlying brain edema, mass effect, and reversible cortical hyperintensity (5, 6, 52). Epidural empyema is

distinguishable from subdural empyema by the specific finding in epidural empyema of a hypointense rim of displaced dura interposed between the fluid collection and the underlying brain (52).

Both CT and MRI are excellent studies to detect the sinusitis or mastoiditis which often accompany subdural or epidural empyema (52). Only CT scan can detect congenital or acquired bone defects which might predispose to intracranial infections. MRI, however, may demonstrate septic thrombophlebitis of a perforating vein connecting the sinus mucosa to the epidural and subdural spaces (5).

Cerebritis and Brain Abscess

Cerebritis and brain abscess result either from contiguous spread from a parameningeal focus of infection or from hematogenous dissemination. Hematogenous brain abscess is sometimes secondary to a chronic lung abscess, bronchiectesis, endocarditis, or occasionally congenital heart disease with right-to-left shunt such as patent foramen ovale or tetralogy of Fallot (55). More often brain abscesses result from contiguous infections about the head, including paranasal sinusitis, otitis media and mastoiditis, dental or facial infection, or trauma including surgery. The management of brain abscess has been substantially improved by the use of modern antimicrobials tailored to our better understanding of the microbiology of this disease, but many also acknowledge that the advent of CT scanning and later MRI has been at least as important in lowering the morbidity and mortality of this disease (55-57). Stereotactic needle aspiration guided by CT or MRI allow us to define the microbiology of the abscess and simultaneously drain it (58), which has proven to be a successful and more conservative approach than open drainage.

A brain abscess begins as a focus of cerebritis, which may show only subtle abnormalities on CT or MRI (5), but then progresses over a variable time to the formation of a mature encapsulated abscess, which is readily recognizable by either study (59). Animal studies defined the CT and MRI appearances of these stages of abscess development (60-62) and showed that, but for the higher sensitivity of MRI, the findings by either study were similar and parallelled the imaging characteristics of human brain abscesses. Patients do not often come to diagnosis at the stage of early cerebritis, but when they do, CT scan shows an ill defined low density focal lesion without or with only minimal enhancement. MRI reveals a central focus of hypointensity on T1WI and T2WI (63), although on T2WI there often is white matter edema. Unenhanced T1WI sometimes demonstrates petechial hemorrhage (5, 6). In the unusual syndrome of rhombencephalitis caused by Listeria monocytogenes, in which patients have fever, headache, cranial nerve signs, cerebellar signs, and long-tract motor and/or sensory signs, CT scan often gives normal results, but MRI demonstrates cerebritis in the brain stem characterized by focal asymmetric high signal intensity on T2WI (43, 64, 65). These findings are not specific for listeriosis and are similar to the imaging characteristics of brainstem encephalitis caused presumably by viruses (39) or by acute disseminated encephalomyelitis (66-68).

As late cerebritis evolves into a mature pyogenic abscess, there is characteristic development of a fibrous inflammatory capsule surrounding the central abscess cavity. Most patients with brain abscess are diagnosed at this stage of late cerebritis or early mature abscess and have characteristic imaging findings which are readily demonstrated by CT or MRI. Lesions are typically at the corticomedullary junction, and CT scan shows a ring-enhancing dense capsule surrounding a hypodense necrotic central cavity. The entire lesion lies within an irregular zone of inflammatory edema (5, 6, 43, 59). The capsule tends to be thinnest on its margin bordering the

lateral ventricle (6, 69), perhaps accounting for the tendency of brain abscesses to rupture into the ventricle, with catastrophic results. Occasionally a gas-fluid level is seen in an abscess which has arisen contiguous to sinusitis or a site of trauma or surgery (5).

MRI findings parallel those seen on CT, but with additional interesting features. The central cavity is generally hyperintense to brain on T2WI and hypointense on T1WI. The capsule is isointense or hyperintese to brain on T1WI and enhances with gadolinium (5). It tends to be hypointense, sometimes dramatically so, on T2WI, showing as a dark rim separating the central cavity and the surrounding high signal intensity of inflammatory edema (5, 6, 59, 69, 70). This hypointense capsule on T2WI suggests a focal paramagnetic effect such as might occur with an enhancement agent. Some have suggested that this represents simply proton-poor collagen yielding a poor signal (59), but this hypothesis is inconsistent with the findings on T1WI. Perhaps it is due to paramagnetic effects of microscopic hemorrhage, which would explain the findings on both T1WI and T2WI (6). However, in a study which compared the imaging features and histopathology of surgically proven brain abscesses, Haimes, et al, could not correlate the degree of fibrosis with the MRI findings (70). Neither acute nor subacute hemorrhage was found, and iron stains yielded little evidence for hemosiderin deposition. The authors postulated that the apparent paramagnetic effect that gives rise to the MR characteristics of the capsule occurs because of heterogeneously distributed oxygen-free radicals produced by activated macrophages which were readily demonstrated in the capsule area. This observation was corroborated by similar imaging findings surrounding metastatic tumors and a parenchymal tuberculoma, all of which on histology demonstrated abundant macrophages in their margins (70). The free radical hypothesis remains to be proven.

The comparative CT and MRI findings in cerebritis and brain abscess are summarized in Table 5. Not surprisingly, the MRI features of brainstem abscess closely parallel those of pyogenic abscess elsewhere in the brain (71).

Table 5. Typical CT and MRI findings in cerebritis and brain abscess.

	CT	MRI		Sensitivity
		T1	T2	
Cerebritis	Nl to hypodense	Hypointense	Hyperintense	MR>CT
Abscess:				
Edema	Hypodense	Hypointense	Hyperintense	MR>CT
Capsule	Iso- to hyperdense	Iso- to hyperintense	Hypointense	MR≥CT
	Enhances	Enhances		MR≥CT
Abscess cavity	Hypodense	Hypointense	Hyperintense	MR=CT

CT or MRI can be used to follow the progress of treatment of brain abscess (5, 6). With either study, capsule enhancement is diminished by corticosteroid treatment. Aspiration of the abscess and antibiotic treatment generally result in healing and apparent collapse of the abscess over three to four months in the immunocompetent host but may take longer in immunosuppressed patients. Enhancement of the residual scar fades very slowly and may not fully resolve (5). Such persistent abnormalities on CT or MRI do not in and of themselves indicate failed therapy or a reason to

continue antibiotic therapy beyond its clinically indicated duration (69). A reliable sign of healing is the fading of capsular hypointensity on T2WI which occurs over approximately four months (70).

Granulomatous Infections

The differential diagnosis of granulomatous central nervous system infection is extensive (55), but I shall focus on the commonly encountered imaging characteristics of tuberculosis, cryptococcal meningitis and CNS infections by other endemic mycoses found in the United States, and focally invasive granulomas of the brain exemplified by aspergillosis and zygomycosis.

Tuberculosis

Tuberculosis of the CNS most often manifests as a subacute lymphocytic meningitis, but when tuberculous meningitis is discovered, CT or MRI scans often disclose focal or multifocal small tuberculomas of various sizes (72). More unusually CNS tuberculosis is manifest by focal cerebritis or solitary brain abscess (73) which may be more frequently seen today in association with HIV infection (74). When tuberculosis presents as isolated cerebritis or abscess, its imaging chracteristics mimic those of pyogenic brain abscess as discussed above (6). Chest roentgenograms are usually normal, and the spinal fluid findings are variable, so diagnosis often requires CT- or MRI- guided stereotactic brain biopsy.

Prior to the widespread application of CT scanning, CNS tuberculomas as concomitants of the tuberculous meningitis were seldom diagnosed antemorten. CT scanning resulted in an expanded description of the radiographic features of intracranial tuberculosis, and early case series included descriptions of clinically unsuspected lesions. As a result of the bacillemia of primary tuberculosis or of late miliary tuberculosis, multiple tiny parenchymal brain nodules can sometimes be detected by CT scanning with contrast (75, 76). They are isodense to brain, are inapparent in studies without contrast, and may be clinically silent. More common CT findings in established intracranial tuberculosis have been described by a number of authors prior to the era of comparative studies with MRI (73, 75, 77). These abnormalities most often included hydrocephalus, basilar cistern enhancement, infarcts most often involving the middle cerebral artery distribution, and meningeal and parenchymal tuberculomas (78). In tuberculous meningitis, meningeal enhancement is consistently found in the basal cisterns, most often in the suprasellar cistern. When basal cistern enhancement is demonstrated, hydrocephalus almost always is present (73). Meningeal and parenchymal tuberculomas of various number and size have been discovered by CT scan of patients with or without concomitant tuberculous meningitis (73, 75, 77). Those lesions result either from hematogenous deposition or from local meningovascular invasion of the cortex secondary to meningitis. Tuberculomas on CT scan range in size from several millimeters to several centimeters in size and can involve any part of the brain and subarachnoid space. When small, these granulomas most often appear on CT as round nodules at the corticomedullary junction which enhance brightly with contrast. Larger older lesions begin to resemble pyogenic brain abscess with thick walled capsules and central hypodensity on nonenhanced CT scan. Active granulomas are surrounded by edema, and they show ring-like enhancement of the capsule. Even older stable lesions may calcify, which is best visualized with CT scan, but enhancement around the calcification is much better demonstrated by MRI with gadolinium (79).

MRI has confirmed the findings of CT scanning in intracranial tuberculosis, and, as hoped, has proven even more sensitive and somewhat more specific than CT scanning for this disease. Before the availability of MRI contrast agents, however, MRI seemed somewhat disappointing for evaluation of CNS tuberculosis because of its surprising insensitivity in detecting granulomas (79) or granulomatous basilar meningitis (6). Gadolinium contrast agents changed all that, and enhanced MRI proven repeatedly to be more sensitive than CT scanning in detecting inflammation in the basal cisterns, small parenchymal tuberculous nodules, ischemic infarcts, and focal hemorrhages (72, 78-80). Usually parenchymal tuberculomas are isointense to gray matter on both T1WI and T2WI (79). Sometimes, however, a tuberculoma or its rim is distinctly hypointense on T2WI (79, 81, 82), a feature which resembles that seen with pyogenic brain abscess and has been hypothesized to be a localized paramagnetic effect of oxygen-free radicals associated with macrophages in the granulomatous reaction (70). Others attribute this hypointensity on T2WI to dense granuloma and compressed glial tissue (81).

A recent study by Gupta et al (72), of 26 patients with tuberculous meningitis demonstrated the spectrum of MRI findings but focussed on cranial neuropathies and arteritis caused by tuberculous basilar inflammation. Nine (42%) of their patients had cranial nerve palsies, most commonly the third, fifth, and seventh nerves. MRI demonstrated relevent abnormalities in all, including enhancement and/or thickening of the involved nerve, displacement or compression of the nerve by a tuberculoma, or infarct in the pons or midbrain. In followup, those patients whose neuropathies resolved also showed resolution of enhancement and thickening on MRI, whereas those with brainstem infarcts did not resolve their nerve palsies. Magnetic resonance angiography (MRA) was performed in twenty of their patients, half of whom showed abnormalities. All but one patient with an abnormal MRA also showed infarcts secondary to tuberculous vasculitis. Most infarcts were in the basal ganglia and internal capsule, and over half were hemorrhagic by MRI criteria (72).

Either CT or MRI is a suitable study to follow patients with hydrocephalus and obliteration of the basilar cisterns (5). CT will best MRI in detecting calcifications typical of longstanding disease..

Fungal Infections

A variety of fungi have been described as causes of intracranial infections. Those that cause disease in humans as a yeast form, such as Cryptococcus neoformans, Histoplasma capsulatum, Coccidioides immitis, and Blastomyces dermatitidis more commonly cause hematogenous granulomatous meningitis and only occasionally significant parenchymal granulomas. By comparison, filamentous fungi, which cause human disease as a hyphal form can infect the brain either hematogenously or by direct perivascular invasion from a mucosal surface and tend to cause focally progressive destructive granulomatous mass lesions with only a minor component of meningitis (83). Candida species cause a variety of syndromes (84) which often resemble pyogenic bacterial infections. Many of these pathogens are considered possible opportunists, although any of them can cause CNS disease in a normal host. AIDS, intravenous drug use, cancer chemotherapy, organ transplantation (especially bone marrow transplantation), immunosuppressive therapy, parenteral nutrition, iron chelation therapy, and diabetes mellitus may predispose to CNS infection with one or more of these fungi (85).

Cryptococcus neoformans

Cryptococcus disseminates hematogenously to cause subacute or chronic meningitis or rarely a focal parenchymal granuloma known as a cryptococcoma (86). Results of imaging studies in

cryptococcal meningitis are generally normal. Meningeal enhancement is only rarely seen on CT scan, although hydrocephalus is easily detected and is fairly common (87). MRI, like CT scan, can detect parenchymal granulomas, most commonly in the basal ganglia, thalamus, and midbrain, and MRI tends to be the more sensitive technique (87-89). Lesions tend to be small, are hypointense on T1WI, hyperintense on T2WI, and may, but not always, show enhancement by either CT or MRI (88, 90). These nonenhancing nodules or larger masses have been referred to as gelatinous pseudocysts of cryptococci which provoke little inflammatory response (89). A similar type of lesion by CT and MRI characteristics has been described in the basal ganglia in the distribution of the perforating arteries and corresponds to the pathologic finding of cystic collections of cryptococci which have spread directly from the basal meninges into the Virchow-Robin spaces from which the microorganisms can locally invade the brain substance (91). This phenomenon is best demonstrated by T2WI as a hyperintensity in the distribution of these arteries, is more readily appreciated by MRI than CT, and when seen may be specific for cryptococcosis (87, 91).

Coccidioides immitis

Coccidioidomycosis on the CNS is most often manifest as chronic meningitis, although cerebritis, miliary granulomas, ventriculitis, and hydrocephalus may also occur (83). Coincident extraneural disease of skin, lungs, and the skeletal systems may be additional clues to diagnosis (86). The imaging characteristics are not specific and are consistent with other causes of chronic meningitis or parenchymal granulomas as might be seen with tuberculosis.

Blastomyces dermatitidis

Involvement of the CNS by blastomycosis is rare, most often seen as meningitis or parenchymal granulomas or abscesses. Again, the imaging characteristics are not distinctive from other chronic granulomatous or pyogenic infections of the CNS (87). Extraneural disease of skin, bones, lungs, or urinary tract is almost always simultaneously present, and occasionally CNS infection may complicate contiguous blastomycosis of the paranasal sinuses (92).

Histoplasma capsulatum

Histoplasmosis of the CNS also may present as chronic meningitis or miliary granulomas, but occasionally a larger histoplasmoma may occur. On MRI the histoplasmoma may show a rim of hypointensity on T2WI, surrounded by vasogenic edema, a finding not unlike mature brain abscesses or tuberculomas as discussed above (93). The imaging characteristics of CNS histoplasmosis are thus not distinct from other chronic CNS infections.

Filamentous Fungal Infections

Filamentous fungal infections of the CNS are most commonly caused by Aspergillus species or zygomycetes. They are generally encountered as opportunistic infections complicating organ transplantation (94), intravenous drug use (95), neutropenia, hematologic neoplasia, head trauma, neurosurgical procedures, or corticosteroid therapy but may infect the normal host (83). Invasive rhinocerebral zygomycosis (mucormycosis) also may complicate diabetic ketoacidosis or iron chelation therapy, and the more unusual Pseudallescheria boydii is sometimes a consequence of near-drowning (96). Regardless of the variances in predisposition, aspergillosis and zygomycosis invade the central nervous system in similar ways, either by direct invasion from nasal or sinus mucosa along vascular pathways or by hematogenous spread, usually from a pulmonary site of inoculation. In either case the CNS lesion is generally an expanding space-occupying inflammatory infarct or cerebritis which may be dry or hemorrhagic and whose pathogenesis is

related to the propensity of these fungi to invade arteries. It is unusual for a well-contained circumscribed granuloma or abscess to form, although these may occur with aspergillosis in immunocompetent patients whose infection spreads directly from the sinuses or middle ear. When well formed abscesses occur, their imaging characteristics cannot be distinguished from pyogenic brain abscesses, appearing on CT as a ring-enhancing mass surrounded by vasogenic edema. Cavernous sinus thrombosis and contiguous inflammatory changes in the orbits or paranasal sinuses are often seen (87, 97, 98). On MRI the abscess may exhibit a hypointense rim on T2WI suggesting a paramagnetic effect as has been described with pyogenic abscesses and tuberculomas (99). However, the margin of an aspergillus abscess tends to be hemorrhagic, and it is likely the paramagnetic effects of this blood in addition to macrophage infiltration that accounts for this hypointense rim in T2WI.

Contiguous fungal sinusitis, which appears dense on CT scan, may show striking hypointensity on MRI with T2WI, which is distinctly unlike the high intensity signal generally seen in allergic or bacterial sinusitis. Zinreich, et al, secured concretions from cases of fungal sinusitis with these imaging characteristics and tested these concretions for iron, manganese, and magnesium by furnace atomic absorption spectroscopy (100). Iron and manganese, which are paramagnetic, were both found in higher concentration in fungal concretions compared to secretions from bacterial sinus infection. Calcium was also found on stain, but hemosiderin was not. The authors concluded that the hypointensity on T2WI of fungal sinusitis may be accounted for by the presence of these paramagnetic elements (100). This imaging characteristic may help discriminate fungal from bacterial sinusitis.

In the immunocompromised host, aspergillosis or zygomycosis tends to spread rapidly and not be readily confined by an inflammatory response. The CT and MRI findings are similar, revealing an expanding mass or infarct, often with a hemorrhagic component (best detected with MRI on noncontrasted T1WI). Because of poor inflammatory response, contrast enhancement may be minimal with either technique (5). One author describes in general terms a subset of bone marrow transplant patients whose cerebral aspergillosis consists of multifocal circumscribed ring-enhancing lesions by CT or MRI and whose disease follows a more benign course than might have been expected for this infection (59).

Although abnormalities of CSF are commonplace in aspergillosis or zygomycosis of the CNS, frank meningitis is unusual, and therefore the CT or MRI features described above for acute or chronic meningitis are not as yet reported.

Herpes Simplex Encephalitis

The imaging characteristics of herpes simplex encephalitis (HSE) have been extensively described and are similar among case series and reviews (5, 6, 69, 101-103). Neonatal HSE is generally not localized like the HSE seen in older children and adults but rather is a diffuse encephalomyelitis ultimately leading to patchy parenchymal necrosis. Early changes on CT scan are often subtle and consist of hypodense areas in the periventricular white matter, sparing the basal ganglia, which may be difficult to distinguish from the normal low density of the neonatal brain. Contrast enhancement is not apparent early in disease, but later the meninges and gyri may enhance (69, 102). Hemorrhagic changes may be seen on CT scan within the first week (69) but are not the rule. End stage disease is characterized on CT by multicystic encephalomalacia, atrophy,

hydrocephalus, and punctate calcifications. None of these neuroimaging findings is considered specific for HSE compared to other neonatal encephalitides (102). With MRI, early neonatal HSE shows loss of gray matter-white matter distinctions and high T2 signal edema of white matter, but these findings may be difficult to appreciate and are nonspecific (69, 103). As disease progresses over the first week confluent necrosis and gyral and meningeal enhancement can be seen (102). Petechial hemorrhages not detected by CT scan can then sometimes be found (104). The end stage changes of atrophy and cystic encephalomalacia are demonstrated as well by MRI as CT, but late calcifications will not be appreciated with MRI (102).

By comparison, HSE in children and adults is almost always localized to the temporal lobes and contiguous brain. It is characterized by subacute necrotizing encephalitis with edema and hemorrhagic infarction (105). Many case series have described the findings on imaging studies and suggest a greater sensitivity of MRI compared to CT in detecting diagnostic abnormalities earlier in disease when antiviral therapy may be more effective (43, 101-103). Early disease is characterized by a low density lesion and subtle mass effect in a temporal lobe on CT scan. Hemorrhage is rarely seen but if present may be specific for HSE. Contrast enhancement is generally delayed for five to seven days into illness. MRI very early in disease shows focal areas in the temporal lobe(s) and contiguous structures of hypointensity on T1WI and hyperintensity on T2WI (5, 106). Hemorrhage is again unusual to see but may be more sensitively detected by T1WI than by CT scan (5, 6, 106). Such focal findings deep in the sylvian fissure, particularly if seen bilaterally, are considered a nearly pathognomonic imaging sign of HSE (5, 102) and are more often detected with MRI than CT scan (101, 102). As with CT, contrast enhancement on MRI is a delayed finding and not generally helpful in early diagnosis. After the first week of disease, MRI is useful but may offer little advantage over CT in diagnosis or in monitoring response to therapy (69, 107). MRI better detects subtle residual abnormalities in the temporal lobes; both techniques easily show atrophy, hydrocephalus, and cystic encephalomalacia; and CT scan shows the occasional end-stage calcification. The comparative typical CT and MRI findings in HSE are summarized in Table 6.

Table 6. Comparative CT and MRI findings in herpes simplex encephalitis

	CT	MRI		Sensitivity
		T1	T2	
Edema	Hypodense	Hypointense	Hyperintense	MR>CT
Enhancement	Late, variable	Late, variable		MR>CT
Hemorrhage	Hyperdense	Hyperintense	Hypointense	MR>CT

Several case reports and small series suggest a role for radioisotope scanning using ^{99m}Tc-HMPAO single-photon emission computed tomography (SPECT) or ^{123}I-IMP in the diagnosis of HSE (108, 109). Several of these cases were scanned only late in disease and thus do not provide information on the comparative value of the scan in early diagnosis. Others have cast doubt on the specificity of these radioisotope techniques and suggest that they remain adjunctive tests for detecting HSE (110-111).

Neurocysticercosis

Cysticercosis is caused by hematogenous spread the larva of the pork tapeworm, Taenia solium, which is endemic in most continents of the earth. Cases transmitted within the United States occur on occasion, but most patients with cysticercosis encountered by physicians in this country have travelled from their native country where transmission is much more frequent because of poor hygiene. Cysticercosis has a predilection to involve striate muscle and central nervous system, perhaps because of the high glycogen content of these tissues (112). Neurocysticercosis may be detected as active or inactive disease depending on the parasite burden; the location and size of the cysts; whether the parasite is alive, degenerating, or dead; and the host's inflammatory response to the parasite (112). Described clinical syndromes include asymptomatic, parenchymal, subarachnoid, intraventricular, spinal, and ocular neurocysticercosis. Combinations of these may also occur.

The neuroimaging characteristics of cysticercosis have been widely described and vary according to the clinical syndromes listed above (5, 6, 102, 112-116). Asymptomatic cysticercosis is common in patients from endemic areas and is discovered either by finding punctate calcifications or cysts on radiographs in asymptomatic patients or as an incidental finding at autopsy. Routine skull roentgenograms or CT scans are the usual studies that detect asymptomatic neurocysticercosis antemortem.

Parenchymal cysticercosis, which is probably the most common clinical presentation (113), is caused by larvae which have settled usually at the junction of gray matter and white matter. Cysts may be present for many years before causing symptoms which, when they occur, may consist of seizures, focal neurologic deficits, mental status deterioration or dementia, an array of other neurologic syndromes, and occasionally acute encephalitis. Symptoms are more likely to occur as the cyst dies, which provokes a localized inflammatory response with resultant edema. Either CT or MRI of stable living cysts show sharply circumscribed cysts which are hypodense on CT and on MRI are hypointense on T1WI and hyperintense on T2WI (resembling CSF). There is no surrounding edema or contrast enhancement by either study. The scolex is not generally visible on CT scan but can be seen on MRI as an isointense or hyperintense mural nodule projecting into the cyst on nonenhanced T1WI. This MRI finding is considered virtually pathognomonic of cysticercosis (6, 115).

As the cysticerci die, usually after years of stability, an acute inflammatory response occurs and may provoke symptoms. Acute parenchymal cysticercosis is detected by CT scan as the typical cystic lesion but with cyst fluid which may appear hyperdense compared to CSF. There is ring enhancement and hypodense edema surrounding the cyst. On MRI, which often detects inflamed cysts more sensitively, cyst fluid is hyperintense to CSF on T1WI; there is nodular or ring-like enhancement with gadolinium; and there is readily apparent inflammatory edema showing a hyperintense signal on T2WI (5, 6, 116). Gadolinium enhancement adds little useful information to the typical MRI findings without it (116). A severe form of this syndrome is seen especially in children and young adults with a high parasite burden, in whom inflammation may present as acute encephalitis which carries a 10% mortality rate (113). By CT scan and perhaps somewhat better by MRI, there can be seen a diffuse pattern of contrast-enhancing nodules or ring-enhanced cysts surrounded by extensive edema. Associated findings in severe disease include mass effect and signs of increased intracranial pressure. Survivors ultimately exhibit on CT scan punctate calcifications typical of dead cysticerci, but illness may take months to subside (102, 113).

Subarachnoid and intraventricular cysticercosis are variants of the same problem and may coexist. These patients, when symptomatic, most often present with headache, meningitis, hydrocephalus, and increased intracranial pressure. Involvement of the basilar cisterns, which is caused by the sterile multicystic racemose form of cysticercosis, is frequently fatal by causing acute hydrocephalus (112). Intraventricular cysts are also quite dangerous. In one series six of forty-six patients with intraventricular cysts died of acute hydrocephalus shortly after diagnosis (114). Intraventricular cysts may also migrate and result in a changing neurologic syndrome (114). Intraventricular and subarachnoid cysts are difficult to see with plain CT but may be detected by metrizamide ventriculography (6, 114). MRI, however, often detects these cysts and has displaced metrizamide ventriculography as the diagnostic study of choice (5, 115). As with parenchymal cysts, the scolex in an intraventricular cyst may be identified on T1WI (6, 115). Large racemose cysts in the basilar cisterns or cerebellopontine angle are sterile although they may continue to enlarge, and a scolex will not be visualized (6, 115).

Spinal Infections

Vertebral Osteomyelitis and Spinal Epidural Abscess

The imaging traits of vertebral osteomyelitis and spinal epidural abscess have been extensively and consistently described, with broad agreement among case series and reviews that include added cases (117-125). MRI has proven much more sensitive than plain radiographs and at least as sensitive as routine radionuclide scans in detecting vertebral osteomyelitis (117, 121), gives better spatial resolution than radionuclide scans, and is superior to CT scanning in detecting spinal cord abnormalities and changes in the cauda equina, meninges, and vertebral bone marrow (121, 124, 125). CT myelography replaced standard myelography in the evaluation of spinal parameningeal infections because of the superior anatomic detail provided by CT, but there remained the risks associated with myelography, including infection, CSF leakage, contrast myelopathy, exascerbating spinal cord compression, and spreading infection to uninvolved spinal compartments (121). MRI, while at least as sensitive as CT-myelography at detecting spinal epidural abscess (126), avoids these hazards of the radiographic procedures and yields more morphologic information with multiplanar imaging (121). For these reasons, the opinions of all authors reviewed are that MRI is the procedure of choice in evaluating infections in and about the spine.

Although spinal epidural abscess can occur following hematogenous dissemination of microorganisms, it is often a complication of contiguous vertebral osteomyelitis or diskitis. Therefore, the imaging findings in vertebral infections will first be reviewed. CT scans of vertebral osteomyelitis may disclose soft tissue phlegmon and obscuration of normal fat planes around the involved vertebral body as well as fragmentation or erosion of the end plates (121). MRI, which detects no signal from bone, nonetheless shows contrasting signals from marrow fat, contiguous soft tissue, CSF and the spinal cord. Initially described in 1985 by Modic, et al, the MRI characteristics of vertebral osteomyelitis have been confirmed and expanded by subsequent authors and include (a) decreased vertebral marrow signal intensity on T1WI because of the T1 lengthening effects of inflammatory edema, (b) loss of the normally distinct signal void of the cortical bone of the end plate, (c) increased signal intensity from the intervertebral disk and end plates on T2WI, (d) loss of the normal signal void (in patients older than 30 years) of the intranuclear cleft in the center of the disk, (e) loss of height of the disk space, and (f) abnormal signal from paraspinous soft tissue (117, 121, 122, 124, 125). Contrast enhancement can be

anticipated in inflamed vertebral marrow, intensifying the signal on T1WI to more approximate the marrow fat signal, perhaps making the lesion appear less conspicuous on T1WI (14, 122, 123). Therefore, fat suppression studies such as STIR sequence images are often performed to heighten the signal contrast between fat and inflammatory edema (124, 127). Usually there is associated contrast enhancement of the disk and of paraspinous and epidural inflammatory tissue, which heightens confidence in the interpretation of infectious spondylitis (120, 122, 123). Findings of inflammatory involvement of vertebral bodies and posterior spinal elements without involvement of contiguous intervertebral disks is suggestive of, though not specific for, tuberculous spondylitis, and approximately 25% of patients with tuberculous spondylitis show hyperintense signal from the contiguous intervertebral disks on T2WI (124, 128). Otherwise, the MR findings in tuberculous spondylitis and fungal or pyogenic infection are not discriminating for a specific class of microorganism (125). Resolution of vertebral osteomyelitis is marked most reliably by return of the normal high intensity marrow fat signal on T1WI (124).

Spinal epidural abscesses have similar imaging characteristics whether they occur as a result of hematogenous or contiguous spread of infection. They may be focal, may involve the entire length of the spine, or may be multiple and noncontiguous (119). T1WI shows an extradural mass compressing the thecal sac and isointense to vertebral marrow or spinal cord. If it follows local extension of a vertebral infection, it obliterates the signal void that normally appears between the vertebral marrow and the spinal cord. On T2WI, the abscess is isointense to CSF and can thus be overlooked because of their apposition (120). Most cases can be readily diagnosed using routine T1- and T2WI (123), but contrast enhancement has been a useful adjunct in making or confirming this diagnosis in some patients and in better delineating the extent of involvement (120, 123, 129). Enhancement may show diffuse homogeneous hyperintensity of a phlegmonous mass of inflamed tissue; linear rim enhancement of the margins of a liquified abscess; or a heterogeneous mixed pattern (120, 123, 124). The pattern of enhancement does not appear to suggest a difference in clinical behavior of the abscess (121). Serial followup of epidural abscess has attempted to correlate MRI findings with clinical outcome (129). In patients who are cured, abnormal findings on MRI subside, but as with successfully treated brain abscess, contrast enhancement may persist long after apparent resolution of clinically apparent disease (129).

Intramedullary Spinal Cord Infections

Myelitis may be acute or chronic and may be caused by a variety of pathogens, including viruses (130, 131), bacteria (132), mycobacteria (133, 134), fungi (135), and parasites (124), and may occur with or without encephalitis (130). Many cases yield no specific etiology but are presumed to be viral or a variant of postviral or postvaccinal acute disseminated encephalomyelitis (68, 136). Patients with AIDS are subject to a variety of spinal myelopathic diseases, including subacute vacuolar myelopathy and acute myelitis caused by CMV, HSV-II, or other opportunistic pathogens (42, 124, 137, 138).

Before the advent of MRI, routine or CT myelography were the only diagnostic imaging studies for myelitis, and findings were limited to the occasional demonstration of spinal cord swelling (125). MRI, with its ability to distinguish intramedullary lesions, has become the clear choice in evaluating spinal cord lesions, and gadolinium contrast agents have further assisted in definition and differential diagnosis of spinal myelopathies.

MRI demonstrates not only spinal cord enlargement if it is present but also signal changes within the cord in the region(s) of involvement (139, 140). T1WI may show hypointensity due to edema

or a subtle increase in intensity which has been attributed to petechial hemorrhages. High signal edema in the same distribution is seen on T2WI. Gadolinium enhancement is expected and may show a diffuse, peripheral, speckled, or nodular pattern (140). Contrast-enhanced MRI may also be helpful in the diagnosis of pyogenic (132) or granulomatous (124, 133-135) myelitis, but the imaging characteristics of these infections are not unlike those seen in viral myelitis. Noninfectious causes of intramedullary disease such as neoplasms are also readily detected by MRI and must be considered in the differential diagnosis of myelitis (124, 141).

HIV Infection and AIDS

Neurological complications of HIV infection and AIDS are common, with infections, neoplasia, or other CNS disease ultimately affecting the majority of patients. A wealth of literature has grown out of the variety of neurological diseases suffered by patients with AIDS, but I shall review the neuroimaging characteristics of only a selection of the most common diffuse or focal CNS diseases which physicians are likely to encounter, specifically HIV encephalopathy, progressive multifocal leukoencephalopathy (PML), toxoplasmosis, primary CNS lymphoma, and cytomegalovirus (CMV) encephalitis. Patients with AIDS frequently present with cryptococcal meningitis and occasionally with CNS tuberculosis or other granulomatous diseases, but the spectrum of imaging findings in these illlnesses do not differ in AIDS from those found in other hosts and have already been reviewed.

Early in the AIDS epidemic it became apparent that CT scanning was a key procedure in evaluating HIV patients with neurological complaints. Mass lesions, which were most commonly toxoplasmosis but occasionally lymphoma or other diseases, were detected with relative ease (142-144), and the use of double dose intravenous contrast was suggested as a way to maximize the diagnostic sensitivity for parenchymal disease despite the risk of nephrotoxicity (144). In the mid-1980's, with the advent of MRI, early comparative studies began to suggest that MRI, even before gadolinium contrast agents were available, offered sensitivity in detecting CNS diseases that until then had escaped discovery by CT scan (43, 145, 146). The principal shortfalls of CT scan were in diffuse CNS lesions without mass effect (such as HIV encephalopathy, PML, or CMV encephalitis) and meningeal disease such as cryptococcosis. MRI was able to demonstrate abnormalities in many of these situations in which CT scans were normal, and the development of gadolinium contrast agents increased dramatically the ability of MRI to detect previously undiscovered lesions. The advantages of MRI in discerning subtle soft tissue contrast of parenchymal lesions and white matter disease, the ability to image the posterior fossa and basilar meninges without bone artifact, and the sensitivity of gadolinium agents in detecting meningeal enhancement and in delineating the margins of focal lesions buried in edema have made MRI the conclusive choice for imaging in patients with AIDS (5, 6, 42, 102, 147, 148).

HIV Encephalopathy

HIV is a neurotropic virus which directly invades the CNS. Early after infection with HIV, a self-limited aseptic meningitis may occur as part of the spectrum of seroconversion syndromes (149). Imaging studies are unnecessary and show normal results. In later stages of HIV disease patients often exhibit a progressive subcortical dementia which has been called HIV encephalopathy or AIDS dementia complex. HIV encephalopathy is characterized clinically by loss of memory and concentration, apathy, psychomotor retardation, and occasionally seizures. Histopathology shows microglial nodules and demyelination (150). The most common neuroimaging finding is cerebral

atrophy, which may begin early in the course of HIV infection (151) and is detected both by CT scan and MRI. As disease progresses, CT may show nonenhancing hypodensity in the white matter, but MRI more sensitively depicts ill-defined diffuse or focal periventricular edema as a hyperintense signal on T2WI. These changes are ususally bilateral but asymmetric, and they most commonly start in the frontal lobes. No enhancement is seen with gadolinium (5, 102, 147, 148). Positron emission tomography (PET) or single-photon emission computed tomography (SPECT) may also show promise in evaluating and monitoring of HIV encephalopathy (152).

Progressive Multifocal Leukoencephalopathy (PML)

Up to 5% of AIDS patients ultimately develop PML after the CD4+ count drops below 200 cells/mm^3 (150) and has been demonstrated to cause subclinical infection much more frequently (153). The JC virus infects oligodendrocytes, resulting in patchy progressive demyelination of white matter. PML presents with various multifocal deficits often including aphasia, visual field deficits, sensorimotor symptoms, and occasionally cerebellar or brainstem deficits. It is untreatable and is fatal over several weeks to months. CT scanning does not detect disease until it is advanced, showing multifocal hypodensity in the subcortical white matter. MRI may demonstrate lesions even before they are clinically apparent (147), and they appear on T2WI or PDWI as focal or multifocal hyperintense patchy white matter disease without mass effect. Disease generally originates in the occipital or parietal lobes, but frontal lobes and cerebellum are also commonly affected (102). In advanced disease, changes in cortical gray matter are also seen (154). Faint marginal contrast enhancement may occasionally be detected at some stage of disease with either CT or MRI (5, 102, 154). Some authors point out that the imaging characteristics of PML are not sufficiently distinguishable from those of HIV encephalopathy to allow a sure diagnosis (42, 102). However, the clinical syndromes are different and when correlated with the imaging results should more surely lend confidence to the diagnosis (150).

Toxoplasmosis

Toxoplasma gondii is the cause of the most commonly encountered focal CNS complication of AIDS and has been recognized since early in the AIDS epidemic (142). Cerebral toxoplasmosis occurs in 5-20% of late AIDS patients and in perhaps one-third of AIDS patients who are seropositive for anti-toxoplasma antibodies. It may rarely cause meningitis or diffuse encephalitis (102, 147). Typically, however, it causes unifocal (approximately 30-40% of cases) or more commonly multifocal mass-like abscesses (155, 156). Patients with toxoplasmosis present in late stage AIDS with focal cerebral symptoms and signs, seizures, headache, and often fever evolving over several days (150). MRI is broadly recognized as more sensitive than CT scan at detecting the typical abscesses, which most commonly involve the basal ganglia but may occur at the gray-white junctions, cerebellum, or brainstem (5, 6, 42, 147). Noncontrast CT shows foci of low density with mass effect, and these usually enhance in a nodular or ring-like pattern. Double dose intravenous contrast administration followed by delayed scanning is the most sensitive method of detecting these lesions with CT (144). However, MRI detects more lesions and at an earlier stage. On T1WI they appear as focal low intensity, and mass effect is easily recognized. On PDWI and T2WI, the abscesses are generally hyperintense and surrounded by higher signal edema. They enhance with gadolinium, which also detects the interface between the toxoplasma abscess and the inflammatory edema, thus effectively localizing the lesion for possible biopsy. Rarely, the toxoplasma abscess will be hemorrhagic (147), and this should be demonstrable on the uncontrasted T1WI. Either CT or MRI is useful in following patients on treatment, with improvement in imaging findings generally occurring within several days to weeks and parallelling clinical response to antitoxoplasmal therapy (5, 155, 156).

Primary CNS Lymphoma

Primary CNS lymphoma in AIDS is less frequently encountered than toxoplasmosis but remains the first alternative diagnosis in patients late in AIDS who have focal CNS symptoms and parenchymal masses demonstrated by CT or MRI (150, 157-159). Its incidence is increasing, probably as a result of more effective management of the opportunistic infections of AIDS, thus allowing patients to survive long enough to develop lymphoma (159). As with toxoplasmosis, CNS lymphoma occurs at a stage of marked CD4+ cell depletion but evolves more slowly. Symptoms and signs vary with the location of the lesions but are generally subcortical intellectual deterioration and focal motor deficits. Lesions are found on scan most commonly in the periventricular white matter but can occur anywhere in the brain, brainstem, or cerebellum. Whereas in non-AIDS patients, CNS lymphoma is typically hyperdense and shows homogeneous contrast enhancement, in AIDS patients lymphoma tends to be hypodense (hyperdense in one-third) and display nodular or ring-like enhancement (157-159). Approximately 10% are not detected by CT (159). With MRI, noncontrasted T1WI shows a low intensity signal associated with mass effect. On T2WI, the usual lesion is centrally hypointense but surrounded by high signal intensity edema which may not be as striking as the edema surrounding toxoplasma lesions. A pattern of focal periventricular lesions with subependymal spread or ventricular encasement is more likely lymphoma than toxoplasmosis (158) as does a pattern of multiple or very large (148, 157) lesions involving both white matter and deep gray matter (148). A target-like lesion with central hypointensity on T2WI can be seen with either toxoplasmosis or lymphoma, and both may enhance with gadolinium on T1WI in a nodular or ring-like fashion. Therefore, distinguishing toxoplasmosis from lymphoma by CT scan or MRI is inexact. A recent study suggests that thallium-201 is selectively concentrated by CNS lymphoma lesions, and SPECT scanning accurately distinguishes lymphoma from toxoplasmosis (160). This study awaits reinforcement but could prove to be a step forward in imaging CNS mass lesions in AIDS. Systemic lymphoma in AIDS, when it involves the CNS, usually causes leptomeningeal disease, and CT and MRI are of little help (42).

Cytomegalovirus

Half or more of adults and the great majority of homosexual men have serologic evidence of previous CMV infection which has usually been asymptomatic. Latent CMV infection can reactivate and cause disease when cell-mediated immunity is compromised as occurs in advanced AIDS. Familiar syndromes include retinitis, esophagitis, colitis, adrenalitis, pneumonitis, and encephalitis (161). Encephalopathy ranges from asymptomatic to severe and fatal, and the neuropathology similarly covers a spectrum from rare CMV inclusions without inflammation to necrotizing ependymitis and meningoencephalitis (162). Coinfection with HIV has resulted in uncertainty in ascribing a role to CMV in the pathogenesis of HIV encephalopathy, but both HIV and CMV may be found in proximity to the characteristic microglial nodules seen in this disease (162). Typical symptoms of severe CMV encephalitis include subacute onset of fever, headache, cognitive difficulties, confusion, alterations of personality and alertness, multifocal sensorimotor deficits and cranial nerve (especially extraocular) palsies (161, 163, 164). Coexisting CMV disease elsewhere, most often retinitis, is present in most patients at the time of diagnosis and may already be under treatment when encephalitis develops (163). In autopsy series the extent of neuropathologic changes in the brain are almost invariably more extensive than were suspected antemortem or indeed from the gross appearance of the brain at postmortem examination (162). As in congenital infection, CMV in AIDS is tropic for ependyma and invades centrifugally to damage brain parenchyma and cranial nerve roots (162, 163). Whereas the CSF findings in CMV encephalitis are usually mildly abnormal but nonspecific (162), in one study there was variable

pleocytosis, some with a polymorphonuclear leukocyte predominance, elevated protein in all, and prominent hypoglycorrhachia (163).

Imaging studies are relatively insensitive in detecting early CNS involvement with CMV, with the majority showing either a normal study or mild atrophy and hydrocephalus ex vacuo (162, 165). MRI is more sensitive than CT in detecting more severe CMV disease which is characteristically periventricular (6, 42, 163) but may be multifocal (164). On CT scan, periventricular edema appears as irregular hypodensity and may enhance with contrast (163). MRI demonstrates a rind of periventricular edema as a thick, irregular high intensity signal on T2WI. Multifocal punctate lesions elsewhere in the brain and brainstem may also be detected best with T2WI (164). T1WI may show subtle hypointensity, and the ependymitis and periventriculitis may enhance with gadolinium (5, 147, 148, 163). Several authors note that these same abnormalities may also be seen with toxoplasmosis or lymphoma, so the imaging characteristics of CMV ventriculoencephalitis are not pathognomonic (6, 147, 163).

Acknowledgements

Rob Reeb, MD, and Ward Terry, MD, provided valuable advice and review. Medical Media Production Service at the Dallas Veterans Affairs Medical Center did the photography, figure creation, and slide production. Tanya Sczymanski helped with literature retrieval and did the word processing to produce this syllabus.

References

1. Bushong SC. Magnetic resonance imaging. Physical and biological principles, 2nd Ed. St. Louis: C.V. Mosby Company, 1995.
2. Smith RC, McCarthy S. Physics of magnetic resonance. J Reprod Med 1992; 37:19-26.
3. Smith H-J, Ranallo FN. A non-mathematical approach to basic MRI. Madison, WI: Medical Physics Publishing Corporation, 1989.
4. Villafana T. Fundamental physics of magnetic resonance imaging. Radiol Clin North Am 1988; 26:701-15.
5. Zimmerman RA. Imaging intracranial infections. In: Scheld WM, Whitley RJ, Durack DT, eds. Infections of the central nervous system. New York: Raven Press, Ltd, 1991, p.887-907.
6. Sze G, Zimmerman RA. The magnetic resonance imaging of infections and inflammatory diseases. Radiol Clin North Am 1988; 26:839-59.
7. Bloch F. Nuclear induction. Phys Rev 1946; 70:460-74.
8. Purcell EM, Torvey HC, Pound RV. Resonance absorption by nuclear magnetic moment in a solid. Phys Rev 1946; 69:127.
9. Damadian R. Tumor detection by nuclear magnetic resonance. Science 1971; 171:1151-3.
10. Lauterbur PC. Image formation by induced local interactions: examples employing nuclear magnetic resonance. Nature (London) 1973; 242:190-1.
11. Goldsmith M, Damadian R, Stanford M, Lipkowitz M. NMR in cancer: XVIII. A superconductive NMR magnet for a human sample. Physiol Chem & Phys 1977; 9:105-7.
12. Barkovich AJ, Atlas SW. Magnetic resonance imaging of intracranial hemorrhage. Radiol Clin North Am 1988; 26:801-20.
13. Bradley WG. Hemorrhage and hemorrhagic infections in the brain. Neuroimaging Clin North Am 1994; 4:707-32.
14. Saini S, Modic MT, Hamm B, Hahn PF. Advances in contrast enhanced MR imaging. AJR 1991; 156:235-54.
15. Watson AD, Rocklage SM, Carvlin MJ. Contrast agents. In Stark DD, Bradley WG, eds. Magnetic resonance imaging, 2nd ed. St. Louis: Mosby Year Book, 1992, p.372-437.
16. Elster AD, Moody DM, Ball MR, Laster DW. Is Gd-DTPA required for routine cranial MR imaging? Radiology 1989; 173:231-8.
17. Schwaighofer BW, Klein MV, Wesbey G, Hesselink JR. Clinical experience with routine Gd-DTPA administration for MR imaging of the brain. J Comput Assist Tomogr 1990; 14:11-7.
18. Price AC, Runge VM, Nelson KL. CNS-nonneoplastic disease. In: Runge VM, ed. Enhanced magnetic resonance imaging. St. Louis: C.V. Mosby, 1989, p.178-92.
19. Hendrick RE, Haacke EM. Basic physics of MR contrast agents and maximization of image contrast. JMRI 1993; 3:137-48.
20. Russell EJ, Geremia GK, Johnson CE, Huckman MS, Ramsey RG, Washburn-Bleck J, Turner DA, Norusis M. Multiple cerebral metastases: detectability with Gd-DTPA-enhanced MR imaging. Radiology 1987; 165: 609-17.
21. Tweedle MF. Physicochemical properties of gadoteridol and other magnetic resonance contrast agents. Invest Radiol 1992 (suppl): S2-6.
22. Runge VM, Gelblum DY, Pacetti ML, Carolan F, Heard G. Gd-HP-DO3A in clinical MR imaging of the brain. Radiology 1990; 177:393-400.

23. Runge VM, Bradley WG, Brant-Zawadzki MN, Carvlin MJ, et al. Clinical safety and efficacy of gadoteridol: a study in 411 patients with suspected intracranial and spinal disease. Radiology 1991; 181:701-9.
24. Wolf GL. Current status of MR imaging contrast agents: special report. Radiology 1989; 172:709-10.
25. Kanal E, Shellock FG, Talagala L. Safety considerations in MR imaging. Radiology 1990; 176:593-606.
26. Barnothy MF, ed. Biological effects of magnetic fields. New York: Plenum Press, 1964.
27. Budinger TF. Nuclear magnetic resonance (NMR) in vivo studies: known thresholds for health effects. J Comput Assist Tomogr 1981; 5:800-11.
28. Budinger TF, Fischer H, Hentschel D, Reinfelder H, Schmitt F. Physiological effects of fast oscillating magnetic field gradients. J Comput Assist Tomogr 1991; 15:909-14.
29. Reid A, Smith FW, Hutchison JMS. Nuclear magnetic resonance imaging and its safety implications: follow-up of 181 patients. Brit J Radiol 1982; 55:784-6.
30. National Radiological Protection Board. Revised guidance on acceptable limits of exposure during nuclear magnetic resonance clinical imaging. Brit J Radiol 1983; 56:974-7.
31. Shellock FG, Crues JV. Temperature, heart rate, and blood pressure changes associated with clinical MR imaging at 1.5T. Radiology 1987; 163:259-62.
32. Shellock FG, Slimp GL. Severe burn of the finger caused by using a pulse oximeter during MR imaging. AJR 1989; 153:1105.
33. Shellock FG. MR imaging of metallic implants and materials: a compilation of the literature. AJR 1988; 151:811-4.
34. Kent DL, Haynor DR, Longstreth WT, Larson EB. The clinical efficacy of magnetic resonance imaging in neuroimaging. Ann Intern Med 1994; 120:856-71.
35. Kent DL, Larson EB. Magnetic resonance imaging of the brain and spine. Is clinical efficacy established after the first decade? Ann Intern Med 1988; 108:402-24.
36. American College of Physicians. Magnetic resonance imaging of the brain and spine. Ann Intern Med 1988; 108:474-6.
37. American College of Physicians. Magnetic resonance imaging of the brain and spine: a revised statement. Ann Intern Med 1994; 120:872-5.
38. Davidson HD, Steiner RE. Magnetic resonance imaging in infections of the central nervous system. AJNR 1985; 6:499-504.
39. Furman JM, Brownstone PK, Baloh RW. Atypical brainstem encephalitis: magnetic resonance imaging and oculographic features. Neurology 1985; 35:438-40.
40. Zimmerman RA, Bilaniuk LT, Sze G. Intracranial infection. In: Brant-Zawadski M, Norman D, eds. Magnetic resonance imaging of the central nervous system. New York: Raven Press, 1987, p.235-57.
41. Tarr RW, Edwards KM, Kessler RM, Kulkarni MV. MRI of mumps encephalitis: comparison with CT evaluation. Pediatr Radiol 1987; 17:59-62.
42. Sze G, Brant-Zawadzki MN, Norman D, Newton TH. The neuroradiology of AIDS. Semin Roentgenol 1987; 22:42-53.
43. Schroth G, Kretzschmar K, Gawehn J, Voigt K. Advantage of magnetic resonance imaging in the diagnosis of cerebral infections. Neuroradiology 1987; 29:120-6.
44. Chang KH,Han MH, Roh JK, Kim IO, Han MC, Kim C. Gd-DTPA-enhanced MR imaging of the brain in patients with meningitis: comparison with CT. AJNR 1990; 11:69-76.

45. Bilaniuk LT, Zimmerman RA, Brown L, Yoo HJ, Goldberg HI. Computed tomography in meningitis. Neuroradiology 1978; 16:13-4.
46. Mathews VP, Kuharik MA, Edwards MK, D'Amour PG, Azzarelli B, Dreesen RG. Gd-DTPA-enhanced MR imaging of experimental bacterial meningitis: evaluation and comparison with CT. AJNR 1988; 9:1045-50.
47. Roos KL, Tunkel AR, Scheld WM. Acute bacterial meningitis in children and adults. In: Scheld WM, Whitley RJ, Durack DT, eds. Infections of the central nervous system. New York: Raven Press, Ltd, 1991, p.335-424.
48. McCracken GH, Jr., Mize SG, Threlkeld N. Intraventricular gentamicin therapy in gram-negative bacillary meningitis of infancy. Report of the Second Neonatal Meningitis Cooperative Study Group. Lancet 1980; 1:787-91.
49. Wirt TC, McGee ZA, Oldfield EH, Meacham WF. Intraventricular administration of amikacin for complicated gram-negative meningitis and ventriculitis. J Neurosurg 1979; 50:95-9.
50. Wright PF, Kaiser AB, Bowman CM, McKee KT, Jr., Trujillo H, McGee ZA. The pharmacokinetics and efficacy of an aminoglycoside administered into the cerebral ventricles in neonates: implications for further evaluation of this route of therapy in meningitis. J Infect Dis 1981; 143:141-7.
51. Helfgott DC, Weingarten K, Hartman BJ. Subdural empyema. In: Scheld WM, Whitley RJ, Durack DT, eds. Infections of the central nervous system. New York: Raven Press, Ltd, 1991, p.487-98.
52. Weingarten K, Zimmerman RD, Becker RD, Heier LA, Haimes AB, Deck MDF: Subdural and epidural empyemas: MR imaging. AJNR 1989; 10:81-7.
53. Tsuchiya K, Makita K, Furui S, Kusano S, Inoue Y. Contrast-enhanced magnetic resonance imaging of sub- and epidural empyemas. Neuroradiology 1992; 34:494-6.
54. Gellin BG, Weingarten K, Gamache FW, Hartman BJ. Epidural abscess. In: Scheld WM, Whitley RJ, Durack DT, eds. Infections of the central nervous system. New York: Raven Press, Ltd, 1991, p.499-514.
55. Luby JP. Southwestern internal medicine conference: infections of the central nervous system. Am J Med Sci 1992; 304:379-91.
56. Rosenblum ML, Hoff JT, Norman D, Weinstein PR, Pitts L. Decreased mortality from brain abscess since the advent of computerized tomography. J Neurosurg 1978; 49:658-68.
57. Ferriero DM, Derechin M, Borg BO. Outcome of brain-abscess treatment in children-reduced morbidity with neuroimaging. Neurology 1986; 36:149.
58. Nauta HJW, Contreras FL, Weiner RL, Crofford MJ. Brain stem abscess managed with computed tomography-guided stereotactic aspiration. Neurosurgery 1987; 20:476-80.
59. Enzmann DR. Magnetic resonance imaging update on brain abscess and central nervous system aspergillosis. In: Remington JS, Swartz MN, eds. Current clinical topics in infectious diseases, 13. Boston: Blackwell Scientific Publications, 1989, p.269-92.
60. Brant-Zawadzki M, Enzmann DR, Placone RC, Sheldon P, Britt RH, Brasch RC, Crooks LA. NMR imaging of experimental brain abscess: comparison with CT. AJNR 1983; 4:250-3.
61. Gross RI, Wolf G, Biery D, McGrath J, Kundel H, Aronchik J, Zimmerman RA, Goldberg HI, Bilaniuk LT. Gadolinium enhanced nuclear magnetic resonance images of experimental brain abscess. J Comput Assist Tomogr 1984; 8:204-7.

62. Runge VM, Clanton JA, Price AC, Herzer WA, Allen JH, Partain CL, James AE. Evaluation of contrast-enhanced MR imaging in a brain-abscess model. AJNR 1985; 6:139-47.
63. Hatta S, Mochizuki H, Kuru Y, Miwa H, Kondo T, Mori H, Mizuno Y. Serial neuroradiological studies in focal cerebritis. Neuroradiology 1994; 36:285-8.
64. Just M, Kramer G, Higer HP, Thomke F, Pfannenstiel P. MRI of Listeria rhombencephalitis. Neuroradiology 1987; 29:401-2.
65. Armstrong RW, Fung PC. Brainstem encephalitis (rhombencephalitis) due to Listeria monocytogenes: case report and review. Clin Infect Dis 1993; 16:689-702.
66. Atlas SW, Grossman RI, Goldberg HI, Hackney DB, Bilaniuk LT, Zimmerman RA. MR diagnosis of acute disseminated encephalomyelitis. J Comput Assist Tomogr 1986; 10:798-801.
67. Caldemeyer KS, Harris TM, Smith RR, Edwards MK. Gadolinium enhancement in acute disseminated encephalomyelitis. J Comput Assist Tomogr 1991; 15:673-5.
68. Caldemeyer KS, Smith RR, Harris TM, Edwards MK. MRI in acute disseminated encephalomyelitis. Neuroradiology 1994; 36:216-20.
69. Buff BL, Mathews VP, Elster AD. Bacterial and viral parenchymal infections of the brain. Top Magn Reson Imaging 1994; 6:11-21.
70. Haimes AB, Zimmerman RD, Morgello S, Weingarten K, Becker RD, Jennis R, Deck MDF. MR imaging of brain abscesses. AJNR 1989; 10:279-91.
71. Carpenter JL. Brain stem abscesses: cure with medical therapy, case report, and review. Clin Infect Dis 1994; 18:219-26.
72. Gupta RK, Gupta S, Singh D, Sharma B, Kohli A, Gujral RB. MR imaging and angiography in tuberculous meningitis. Neuroradiology 1994; 36:87-92.
73. Jinkins JR. Computed tomography of intracranial tuberculosis. Neuroradiology 1991; 33:126-35.
74. Barnes PF, Bloch AB, Davidson PT, Snider DE. Tuberculosis in patients with human immunodeficiency virus infection. N Engl J Med 1991; 324:1644-50.
75. Rovira M, Romero F, Torrent O, Ibarra B. Study of tuberculous meningitis by CT. Neuroradiology 1980; 19:137-41.
76. Witham RR, Johnson RH, Roberts DL. Diagnosis of miliary tuberculosis by cerebral computerized tomography. Arch Intern Med 1979; 139:479-80.
77. Draouat S, Abdenabi B, Ghanem M, Bourjat P. Computed tomography of cerebral tuberculoma. J Comput Assist Tomogr 1987; 11:594-7.
78. Offenbacher H, Fazekas F, Schmidt R, Kleinert R, Payer F, Kleinert G, Lechner H. MRI in tuberculous meningoencephalitis: report of four cases and review of the neuroimaging literature. J Neurol 1991; 238: 340-4.
79. Chang K-H, Han M-H, Roh J-K, Kim I-O, Han M-C, Choi K-S, Kim C-W. Gd-DTPA enhanced MR imaging in intracranial tuberculosis. Neuroradiology 1990; 32:19-25.
80. Villoria MF, de la Torre J, Fortea F, Munoz L, Hernandez T, Alarcon JJ. Intracranial tuberculosis in AIDS: CT and MRI findings. Neuroradiology 1992; 34:11-4.
81. Gupta RK, Jena A, Sharma A, Guha DK, Khushu S, Gupta AK. MR imaging of intracranial tuberculosis. J Comput Assist Tomogr 1988; 12:280-5.
82. Kioumehr F, Dadsetan MR, Rooholamini SA, Au A. Central nervous system tuberculosis: MRI. Neuroradiology 1994; 36:93-6.
83. Sepkowitz K, Armstrong D. Space-occupying fungal lesions of the central nervous system. In: Scheld WM, Whitley RJ, Durack DT, eds. Infections of the central nervous system. New York: Raven Press, Ltd, 1991, p.741-64.

84. Lipton SA, Hickey WF, Morris JH, Loscalzo J. Candidal infections in the central nervous system. Am J Med 1984; 76:101-8.
85. Perfect JR, Durack DT. Pathogenesis and pathophysiology of fungal infections of the central nervous system. In: Scheld WM, Whitley RJ, Durack DT, eds. Infections of the central nervous system. New York: Raven Press, Ltd, 1991, p.693-702.
86. Tucker T, Ellner JJ. Chronic meningitis. In: Scheld WM, Whitley RJ, Durack DT, eds. Infections of the central nervous system. New York: Raven Press, Ltd, 1991, p.703-28.
87. Ostrow TD, Hudgins PA. Magnetic resonance imaging of intracranial fungal infections. Top Magn Reson Imaging 1994; 6:22-31.
88. Takasu A, Taneda M, Otuki H, Okamoto Y, Oku K. Gd-DTPA-enhanced MR imaging in cryptococcal meningoencephalitis. Neuroradiology 1991; 33:443-6.
89. Popovich MJ, Arthur RH, Helmer E. CT of intracranial cryptococcosis. AJNR 1990; 11:139-42.
90. Mathews VP, Alo PL, Glass JD, Kumar AJ, McArthur JC. AIDS-related cryptococcosis: radiologic-pathologic correlation. AJNR 1992; 13:1477-86.
91. Wehn SM, Heinz ER, Burger PC, Boyko OB. Dilated Virchow-Robin spaces in cryptococcal meningitis associated with AIDS: CT and MR findings. J Comput Assist Tomogr 1989; 13:756-62.
92. Angtuaco EEC, Angtuaco EJC, Glasier CM, Benitez WI. Nasopharyngeal and temporal bone blastomycosis: CT and MR findings. AJNR 1991; 12:725-8.
93. Dion FM, Venger BH, Landon G, Handel SF. Thalamic histoplasmoma: CT and MR imaging. J Comput Assist Tomogr 1987; 11:193-5.
94. Hagensee ME, Bauwens JE, Kjos B, Bowden RA. Brain abscess following marrow transplantation: experience at the Fred Hutchinson Cancer Research Center, 1984-1992. Clin Infect Dis 1994; 19:402-8.
95. Stave GM, Heimberger T, Kerkering TM. Zygomycosis of the basal ganglia in intravenous drug users. Am J Med 1989; 86:115-7.
96. Berenguer J, Diaz-Mediavilla J, Urra D, Munoz P. Central nervous system infection caused by Pseudallescheria boydii: case report and review. Rev Infect Dis 1989; 11:890-6.
97. Press GA, Weindling SM, Hesselink JR, Ochi JW, Harris JP. Rhinocerebral mucormycosis: MR manifestations. J Comput Assist Tomogr 1988; 12:744-9.
98. Yousem DM, Galetta SL, Gusnard DA, Goldberg HI. MR findings in rhinocerebral mucormycosis. J Comput Assist Tomogr 1989; 13:878-82.
99. Cox J, Murtagh R, Wilfong A, Brenner J. Cerebral aspergillosis: MR imaging and histopathologic correlation. AJNR 1992; 13:1489-92.
100. Zinreich SJ, Kennedy DW, Malat J, Curtin HD, Epstein JI, Huff LC, Kumar AJ, Johns ME, Rosenbaum AE. Fungal sinusitis: diagnosis with CT and MR imaging. Radiology 1988; 169:439-44.
101. Schroth G, Gawehn J, Thron A, Vallbracht A, Voigt K. Early diagnosis of herpes simplex encephalitis by MRI. Neurology 1987; 37:179-83.
102. Jordan J, Enzmann DR. Encephalitis. Neuroimag Clin North Am 1991; 1:17-38.
103. Tien RD, Felsberg GL, Osumi AK. Herpesvirus infections of the CNS: MR findings. AJR 1993; 161: 167-76.
104. Enzmann DR, Chang Y, Augustyn G. MR findings in neonatal herpes simplex encephalitis type II. J Comput Assist Tomogr 1990; 14:453-7.

105. Whitley RJ, Schlitt M. Encephalitis by herpesviruses, including B virus. In: Scheld WM, Whitley RJ, Durack DT, eds. Infections of the central nervous system. New York: Raven Press, Ltd., 1991, p.41-86.
106. Demaerel P, Wilms G, Robberecht W, Johannik K, Van Hecke P, Carton H, Baert AL. MRI of herpes simplex encephalitis. Neuroradiology 1992; 34:490-3.
107. Lester JW, Carter MP, Reynolds TL. Herpes encephalitis: MR monitoring of response to acyclovir therapy. J Comput Assist Tomogr 1988; 12:941-3.
108. Launes J, Lindroth L, Liewendahl K, Nikkinen P, Brownell AL, Iivanainen M. Diagnosis of acute herpes simplex encephalitis by brain perfusion single photon emission computed tomography. Lancet 1988; 1:1188-91.
109. Schmidbauer M, Podreka I, Wimberger D, Oder W, Koch G, Wenger S, Goldenberg G, Asenbaum S, Deecke L. SPECT and MR imaging in herpes simplex encephalitis. J Comput Assist Tomogr 1991; 15:811-5.
110. Pennell DJ, O'Doherty MJ, Page C, Nunan TO, Croft DN, ^{99m}Tc-HMPAO scanning in focal encephalitis. Lancet 1988; 2:104-5.
111. Klapper PE, Cleator GM, Lewis AG. ^{99m}Tc-HMPAO scanning in focal encephalitis. Lancet 1988; 2:105.
112. Cameron ML, Durack DT. Helminthic infections of the central nervous system. In: Scheld WM, Whitley RJ, Durack DT, eds. Infections of the central nervous system. New York: Raven Press, Ltd., 1991, p.825-58.
113. Rodriguez-Carbajal J, Salgado P, Gutierrez-Alvarado R, Escobar-Izquierdo A, Aruffo C, Palacios E. The acute encephalitic phase of neurocysticercosis: computed tomographic manifestations. AJNR 1983; 4:51-5.
114. Zee C, Segall HD, Apuzzo MLJ, Ahmadi J, Dobkin WR. Intraventricular cysticercal cysts: further neuroradiologic observations and neurosurgical implications. AJNR 1984; 5:727-30.
115. Suss RA, Maravilla KR, Thompson J. MR imaging of intracranial cysticercosis: comparison with CT and anatomopathologic features. AJNR 1986; 7:235-42.
116. Chang KH, Lee JH, Han MH, Han MC. The role of contrast-enhanced MR imaging in the diagnosis of neurocysticercosis. AJNR 1991; 12:509-12.
117. Modic MT, Feiglin DH, Piraino DW, Boumphrey F, Weinstein MA, Duchesneau PM, Rehm S. Vertebral osteomyelitis: assessment using MR. Radiology 1985; 157:157-66.
118. Angtuaco EJC, McConnell JR, Chadduck WM, Flanigan S. MR imaging of spinal epidural sepsis. AJNR 1987; 8:879-83.
119. Post MJD, Quencer RM, Montalvo BM, Katz BH, Eismont FJ, Green BA. Spinal infection: evaluation with MR imaging and intraoperative US. Radiology 1988; 169:765-71.
120. Post MJD, Sze G, Quencer RM, Eismont FJ, Green BA, Gahbauer H. Gadolinium-enhanced MR in spinal infection. J Comput Assist Tomogr 1990; 14:721-9.
121. Smith AS, Blaser SI. Infectious and inflammatory processes of the spine. Radiol Clin North Am 1991; 29:809-27.
122. Post MJD, Bowen BC, Sze G. Magnetic resonance imaging of spinal infection. Rheum Dis Clin North Am 1991; 17:773-94.
123. Sandhu FS, Dillon WP. Spinal epidural abscess: evaluation with contrast-enhanced MR imaging. AJNR 1992; 12:1087-93.
124. Sharif HS. Role of MR imaging in the management of spinal infections. AJR 1992; 158:1333-45.

125. Van Tassel P. Magnetic resonance imaging of spinal infections. Top Magn Reson Imaging 1994; 6:69-81.
126. Hlavin ML, Kaminski HJ, Ross JS, Ganz E. Spinal epidural abscess: a ten-year perspective. Neurosurgery 1990; 27:177-84.
127. Bertino RE, Porter BA, Stimac GK, Tepper SJ. Imaging spinal osteomyelitis and epidural abscess with short TI inversion recovery (STIR). AJNR 1988; 9:563-4.
128. Smith AS, Weinstein MA, Mizushima A, Coughlin B, Hayden SP, Lakin MM, Lanzieri CF. MR imaging characteristics of tuberculous spondylitis vs vertebral osteomyelitis. AJNR 1989; 10:619-25.
129. Sadato N, Numaguchi Y, Rigamonti D, Kodama T, Nussbaum E, Sato S, Rothman M. Spinal epidural abscess with gadolinium-enhanced MRI: serial follow-up studies and clinical correlations. Neuroradiology 1994; 36:44-8.
130. Griffin DE. Encephalitis, myelitis, and neuritis. In: Mandell GL, Bennett JE, Dolin R, eds. Principles and practice of infectious diseases, 4th ed. New York: Churchill Livingstone, 1995, p.874-81.
131. Caldas C, Bernicker E, Dal Nogare A, Luby JP. *Case report: transverse myelitis* associated with Epstein-Barr virus infection. Am J Med Sci 1994; 307:45-8.
132. Byrne RW, Von Roenn KA, Whisler WW. Intramedullary abscess: a report of two cases and a review of the literature. Neurosurgery 1994; 35:321-6.
133. Shen W-C, Cheng T-Y, Lee S-K, Ho Y-J, Lee K-R. Disseminated tuberculomas in spinal cord and brain demonstrated by MRI with gadolinium-DTPA. Neuroradiology 1993; 35:213-5.
134. Gupta RK, Gupta S, Kumar S, Kohli A, Misra UK, Gujral RB. MRI in intraspinal tuberculosis. Neuroradiology 1994; 36:39-43.
135. Bazan C, New PZ. Intramedullary spinal histoplasmosis efficacy of gadolinium enhancement. Neuroradiology 1991; 33:190.
136. Chang CM, Ng HK, Chan YW, Leung SY, Fong KY, Yu YL. Postinfectious myelitis, encephalitis, and encephalomyelitis. Clin Exptl Neurol 1992; 29:250-62.
137. Melhem ER, Wang H. Intramedullary spinal cord tuberculoma in a patient with AIDS. AJNR 1992; 13:986-8.
138. Price RW, Brew B. Management of the neurologic complications of HIV infection and AIDS. Infect Dis Clin North Am 1988; 2:359-72.
139. Merine D, Wang H, Kumar AJ, Zinreich SJ, Rosenbaum AE. CT myelography and MR imaging of acute transverse myelitis. J Comput Assist Tomogr 1987; 11:606-8.
140. Gero B, Sze G, Sharif H. MR imaging of intradural inflammatory diseases of the spine. AJNR 1991; 12:1009-19.
141. Sze G, Krol G, Zimmerman RD, Deck MDF. Intramedullary disease of the spine: diagnosis using gadolinium-DTPA-enhanced MR imaging. AJNR 1988; 9:847-58.
142. Kelly WM, Brant-Zawadzki M. Acquired immunodeficiency syndrome: neuroradiologic findings. Radiology 1983; 149:485-91.
143. Whelan MA, Kricheff II, Handler M, Ho V, Crystal K, Gopinathan G, Laubenstein L. Acquired immunodeficiency syndrome: cerebral computed tomographic manifestations. Radiology 1983; 149:477-84.
144. Post MJD, Kursunoglu SJ, Hensley GT, Chan JC, Moskowitz LB, Hoffman TA. Cranial CT in acquired immunodeficiency syndrome: spectrum of diseases and optimal contrast enhancement technique. AJR 1985; 145:929-40.
145. Levy RM, Rosenbloom S, Perrett LV. Neuroradiologic findings in AIDS: a review of 200 cases. AJR 1986; 147:977-83.

146. Post MJD, Sheldon JJ, Hensley GT, Soila K, Tobias JA, Chan JC, Quencer RM, Moskowitz LB. Central nervous system disease in acquired immunodeficiency syndrome: prospective correlation using CT, MR imaging and pathologic studies. Radiology 1986; 158:141-8.
147. Castillo M. Brain infections in human immunodeficiency virus positive patients. Top Magn Reson Imaging 1994; 6:3-10.
148. Benson ML, Laine FJ. Brain imaging in AIDS. South Med J 1995; 88:331-7.
149. Evans BK, Donley DK, Whitaker JN. Neurological manifestations of infection with the human immunodeficiency viruses. In: Scheld WM, Whitley RJ, Durack DT, eds. Infections of the central nervous system. New York: Raven Press, Ltd., 1991, p.201-32.
150. Price RW, Worley JM. Neurological complications of HIV-1 infection and AIDS. In: Broder S, Merigan TC, Jr., Bolognesi D, eds. Textbook of AIDS medicine. Baltimore: Williams & Wilkins, 1994, p.489-505.
151. Raininko R, Elovaara I, Virta A, Valanne L, Haltia M, Valle S-L. Radiological study of the brain at various stages of human immunodeficiency virus infection: early development of brain atrophy. Neuroradiology 1992; 34:190-6.
152. Masdeu JC, Yudd A, Van Heertum RL, Grundman M, Hriso E, O'Connell RA, Luck D, Camli U, King LN. Single photon emission computed tomography in human immunodeficiency virus encephalopathy: a preliminary report. J Nucl Med 1991; 32:1471-5.
153. Quinlivan EB, Norris M, Bouldin TW, Suzuki K, Meeker R, Smith MS, Hall C, Kenney S. Subclinical central nervous system infection with JC virus in patients with AIDS. J Infect Dis 1992; 166:80-5.
154. Von Einsiedel RW, Fife TD, Aksamit AJ, Cornford ME, Secor DL, Tomiyasu U, Itabashi HH, Vinters HV. Progressive multifocal leukoencephalopathy in AIDS: a clinicopathologic study and review of the literature. J Neurol 1993; 240:391-406.
155. Luft BJ, Hafner R, Korzun AH, Leport C, Antoniskis D, et al. Toxoplasmic encephalitis in patients with the acquired immunodeficiency syndrome. N Engl J Med 1993; 329:995-1000.
156. Renold C, Sugar A, Chave J-P, Perrin L, Delavelle J, Pizzolato G, Burkhard P, Gabriel V, Hirschel B. Toxoplasma encephalitis in patients with the acquired immunodeficiency syndrome. Medicine 1992; 71:224-39.
157. Kupfer MC, Zee C-S, Colletti PM, Boswell WD, Rhodes R. MRI evaluation of AIDS-related encephalopathy: toxoplasma vs. lymphoma. Magn Reson Imaging 1990; 8:51-7.
158. Dina TS. Primary central nervous system lymphoma versus toxoplasmosis in AIDS. Radiology 1991; 179:823-8.
159. Fine HA, Mayer RJ. Primary central nervous system lymphoma. Ann Intern Med 1993; 119:1093-1104.
160. Ruiz A, Ganz WI, Post MJD, Camp A, Landy H, Mallin W, Sfakianakis GN. Use of thallium-201 brain SPECT to differentiate cerebral lymphoma from toxoplasma encephalitis in AIDS patients. AJNR 1994; 15:1885-94.
161. Drew WL. Cytomegalovirus infection in patients with AIDS. Clin Infect Dis 1992; 14:608-15.
162. Vinters HV, Kwok MK, Ho HW, Anders KH, Tomiyasu U, Wolfson WL, Robert F. Cytomegalovirus in the nervous system of patients with the acquired immune deficiency syndrome. Brain 1989; 112:245-68.
163. Kalayjian RC, Cohen ML, Bonomo RA, Flanigan TP. Cytomegalovirus ventriculoencephalitis in AIDS. Medicine 1993; 72:67-77.

164. Masdeu JC, Small CB, Weiss L, Elkin CM, Llena J, Mesa-Tejada R. Multifocal cytomegalovirus encephalitis in AIDS. Ann Neurol 1988; 23:97-9.
165. Post MJD, Hensley GT, Moskowitz LB, Fischl M. Cytomegalic inclusion virus encephalitis in patients with AIDS: CT, clinical, and pathologic correlation. AJR 1986; 146:1229-34.